USING LIGHT-ACTIVATED EGF TO CONTROL CELL BEHAVIOR USING AUTOMATED INSTRUMENTATION

APPROVED BY SUPERVISORY COMMITTEE

Kevin Luebke, Ph.D.

Matthew Petroll, Ph.D.

Frederick Grinnell, Ph.D.

Liping Tang, Ph.D.

Hanli Liu, Ph.D.

DEDICATION

When I was growing up my family took a lot of family vacations, mostly road trips. Wherever we would drive, after leaving the city, my Dad would quiz us on the things that passed by our windows. The question phrased most often was, “What kind of tree is that?” The most common answer was, “Sycamore.” Not only did I love to learn because of my Dad but I also learned to love science because of him. Or, maybe it was the countless hours my older sister used to pass out homework so she could play ‘teacher.’ Being like any younger sibling, eager to have her attention, it didn’t occur to me to refuse!

That is why I would like to dedicate this work to the unending love, support and inspiration of my family: my Dad who is my hero, my Mom who taught me value in hard work and my sisters who have always been my partners in crime on escapades spanning the world. I would not be who I am today without them.

There is one additional family member who has also played a large role in my life and scholarly studies, my cousin, Harold (Skip) Garner. Not only did he first introduce me to UT Southwestern, but also to my mentor. Skip often credits my Dad for the role he played in Skip’s career and now I would like to credit him for the role he has played in mine.

Twenty-three years ago this summer that I started my first science lab book to document the growth of four baby water turtles I caught at a lake in Missouri while on a family vacation. When I first began the work presented in this document, I was reminded of those moments. I have often experienced the same child-like excitement working in the lab that I did back then, eager to discover and learn new things. That excitement can be attributed in-part to my mentor.

I have had the great privilege of working with an inspiring scientist whose passion for his work is contagious. I will always appreciate the guidance and support my mentor, Kevin Luebke, provided over the duration of this work. I can not imagine a better mentor, he is the ideal role model and my perfect image of what I believe a Ph.D. represents.

USING LIGHT-ACTIVATED EGF TO CONTROL CELL BEHAVIOR USING AUTOMATED INSTRUMENTATION

by

DANIELLE SUZANNE MILLER

DISSERTATION

Presented to the Faculty of the Graduate School of Biomedical Sciences

The University of Texas Southwestern Medical Center at Dallas

In Partial Fulfillment of the Requirements

For the Degree of

DOCTOR OF PHILOSOPHY

The University of Texas Southwestern Medical Center at Dallas

Dallas, Texas

May, 2008

USING LIGHT-ACTIVATED EGF TO CONTROL CELL BEHAVIOR USING AUTOMATED INSTRUMENTATION

DANIELLE SUZANNE MILLER, Ph.D.

The University of Texas Southwestern Medical Center at Dallas, 2008

Supervising Professor: KEVIN J. LUEBKE, Ph.D.

A key interest in cell biology is the ability to control cell behavior, particularly for creating functional assemblies of cells to restore, maintain or enhance tissue and organ function. Success in controlling cell behavior must include techniques that provide signals which influence the organization, growth and activities of cells. Growth factors are naturally occurring proteins that act as external chemical signals and which play a key role in regulation and control of a variety of cellular processes, such as differentiation, proliferation and migration. One of the challenges in controlling these processes using growth factors is the ability to spatially direct their timed release to the cellular environment. Another challenge then becomes the continued ability to influence these

processes with the dynamic flexibility to meet the changing cellular demands during tissue development.

We have developed a technology that uses light-activated epidermal growth factor (EGF) to influence cell behavior. We used peptide synthesis to incorporate a photolabile caging group on a critical residue. The caged-growth factor was inactive until converted with light, which enabled the management of its effects with the precision with which light could be directed. Since the factor was a soluble, diffusible species, it was not limited to a static pattern or substrate. Thus, dynamic control over its mitogenic and chemotactic effects on cell behavior was achieved.

To utilize the light-activated EGF we developed a device for its delivery and activation. The system was a fully automated machine capable of maintaining the strict requirements of cell culture, integrated with components that achieved interchangeable, high resolution patterns, along with an optical system for photo-activating caged growth factors. The instrument was designed, characterized and then used to investigate the effect of light-activated EGF on cell patterning and mobility. Using this device, spatially resolved fibroblast cell patterning and migration were achieved.

Table of Contents

Prior Publications

Miller, Danielle S., Chirayil, Sara, Ball, Haydn L., Luebke, Kevin J., *Manipulating Cell Migration and Proliferation with a Light-Activated Polypeptide*, In preparation.

Miller, Danielle S., Luebke, Kevin J. , *Design and Characterization of Automated Instrumentation for Manipulating Cell Behavior Using Light-Activated Growth Factors*, In preparation.

List of Figures

List of Tables

List of Appendices

List of Definitions

ANOVA – Analysis of Variance

COM – Common

DMD – Digital Micromirror Device

DMEM – Dulbecco's Modified Eagle Medium

EGF – Epidermal Growth Factor

FBS – Fetal Bovine Serum

GAG – glycosaminoglycan

HFF – Human Foreskin Fibroblast

N.O. – Normally Open

N.C. – Normally Closed

PDMS – polydimethylsiloxane

SPIT – Sodium selenite, pyruvate, insulin, transferrin

UVA – Ultraviolet A

CHAPTER ONE

INTRODUCTION AND BACKGROUND

1.1 Tissue Engineering

Construction of three-dimensional assemblages of tissues for repair or replacement is an important engineering challenge. In order for tissue engineering to establish its importance in organ replacement therapies, cell manipulation tools need to be developed to meet the requirements presented by the wide variety of desired tissue types (Martin and Vermette 2005). These tools must meet the basic nutrient supply, waste elimination and mechanical support necessary for cell viability. Engineered technology must also devise a way to influence specific cell behavior in order to create functional tissues that mimic native forms.

1.2 The cellular environment: signals, materials and interactions

The intricate interactions between cell populations and their surrounding matrix are superbly orchestrated endogenously. The extra-cellular matrix provides the structural foundation for tissues. Cells secrete, degrade, modify and move through the matrix, which in turn, exerts tensions that influence cell shape, alignment and phenotype. The cooperative interaction stimulates feedback loops spatially modulated by soluble, diffusible growth factors (Dun 2000). These dynamic interactions present a challenge to duplicate in vitro. In nature, signals are created at the right time and place which they are needed. And, these needs are always changing.

Soluble chemical signals, such as growth factors, provide cues for cells. Cell population density and cell-matrix interactions, such as matrix remodeling and chemotaxis, are among the vast repertoire of functions that growth factors influence. Growth factors also play a role in critical cell functions like differentiation, proliferation and apoptosis. In vivo, these signals are delivered from the surrounding environment to the location they are needed, in vitro, they must be provided. The challenge with delivering these signals in vitro is devising a delivery scheme with the same in vivo precision in space and time; not permanently attached to its surroundings. Technologies that address cell-substrate interactions and enable controlled release of soluble factors have been developed. But a large challenge with substrate engineering, in terms of influencing cell behavior, lies with the inability to revise the surface modification to adapt to the changing cellular environment due to the static nature of the scaffold. This presents a case for the use of soluble signals in tissue engineering. Developing a method to establish both spatial and temporal control of soluble signals presents the opportunity for natural matrices to provide mechanical support to growing cell cultures. This is desirable since it more closely resembles the native environment than technologies using fabricated matrices or signals bound to a surface, and so is a useful tool.

1.3 Light activated molecules and synthesis of light activated growth factors

The closer the strategy is to mimicking the native environment, the higher the degree of influence over controlling cellular behavior will be. A key element of this strategy will be the ability to create chemical signals in the right place, at the right time, as nature does. Much has been done toward this goal with the use of “caged” compounds.

The activity of a chemical signal can be masked by introduction of a photolabile protective group. Photolysis of the protective group releases the non-toxic moiety, producing the active compound in illuminated regions. This strategy has been utilized to control protein expression (Lin, Albanese et al. 2002) and neurotransmission (Furuta, Wang et al. 1999). Light activated proteins have been synthesized by incorporating modified amino acids with photomasked residues (Chang, Niblack et al. 1995; Miller, Silverman et al. 1998; Curley and Lawrence 1999; Marriott and Walker 1999; Pirrung, Drabik et al. 2000; Rothman, Petersson et al. 2005). This tactic provides control over placement of masked side chains. This strategy can be extended to create light-activated growth factors. No light-activated growth factor has been reported to date.

Epidermal growth factor (EGF) is a relatively small protein (53 residues) compared to most growth factors. Synthesis of EGF is possible using routine solid phase methods. Therefore, it is an ideal candidate for creating the first light-activated growth factor. In addition, EGF is known to stimulate several cell behaviors, such as proliferation and migration.

1.31 Synthesis of Light-Activated EGF

Modified amino acids are made by incorporating nitrobenzyl derivatives, which can be removed rapidly and efficiently by photolysis. Glutamate was protected as a photolabile ester via its γ-carboxyilic acid by using (R,S)-1-(3,4-(methylenedioxy)-6-nitrophenyl)

A

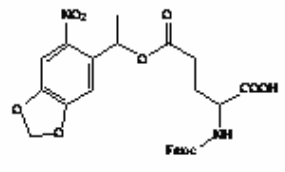

B

NSDSECPLSHDGYCLHDGVCMYIEALDK
YACNCVVGYIG**E**RCQYRDLKWWELR

Figure 1. A. An α-methyl-2-nitropiperonyl glutamate derivative. **B**. Sequence of human EGF. The bold **E** represents glutamate 40, the target for replacement with the caged residue.

alcohol. The caged glutamate was then incorporated at position 40 during solid phase synthesis of EGF to create a light activated version of EGF, Figure 1. This substitution was chosen because it has been reported that mutation of glutamate 40 to glutamine in EGF results in a 4-fold loss of receptor affinity (Campion, Tadaki et al. 1992). As determined by HPLC and MALDI MS, a full length EGF with a single α-methyl-2-nitropiperonyl moiety (m/z=6416) prior to photolysis was produced. The half-life to cleanly deprotect the peptide was 35 seconds (30 mW/cm^2) at 365nm irradiation.

1.4 Instrumentation

Bioreactor devices closely monitor and tightly control environmental and operating conditions such as: pH, temperature, pressure, nutrient supply and waste removal (Martin and Vermette 2005) within a flow cell chamber. The delicate balance between culture and environment greatly influences the characteristics of the developing tissue. For instance, higher shear stress due to mechanical or pulsatile fluid flow conditioning is beneficial to collagen and glycosaminoglycan (GAG) growth, but non-uniform or highly acidic medium can actually inhibit the formation of the extracellular matrix (ECM) (Bilodeau and Mantovani 2006).

To the basic cellular needs, the engineer must integrate components which are easily modified to meet the changing requirements during experimental progression. Engineers have addressed these requirements using a variety of tissue flow cell chamber designs; hollow fiber, fixed wall, rotating wall, stirred tank, etc. Inlet and outlet conditions and flow chamber geometry dictate chamber dimensions necessary for the flow to be stable and laminar (Bakker, van der Plaats et al. 2003). Increased fluid flow can enhance cell attachment or increase shear stress levels to the point of detachment. So

it is critical to evaluate chamber design to establish a velocity profile which will obtain valid observations. Due to its conceptual simplicity, the most common bioreactor style is a parallel plate flow chamber design (Bakker, van der Plaats et al. 2003). In this design, mass transport occurs through slow convective diffusion. These designs lend themselves well to a broad range of materials and applications.

1.5 Research Goals for the Project

The motivation behind the project is to develop a technology for controlling cell behavior using light-activated growth factors. The project had three research goals. The first one was to characterize the biological response of fibroblast cells to light-activated EGF (before and after photolysis). The second goal is to design, construct and characterize an instrument capable of carrying out tissue culture while simultaneously create high resolution photolysis patterns to activate the caged growth factor. The third goal is to utilize the instrument to control cell behavior using starting parameters determined from the biological assays performed in the first goal.

CHAPTER TWO

DETERMINING THE BIOLOGICAL EFFECT OF LIGHT-ACTIVATED EGF ON FIBROBLASTS

2.0 Cellular Response to light-activated EGF

In order to develop an automated platform for creating spatially and temporally resolved cell signaling using light-activated epidermal growth factor (EGF), it was necessary to determine which cell behaviors the caged molecule (before and after photolysis) had influence over and the extent to which the behavior was influenced. Native EGF plays a role in stimulating cell proliferation and migration, so those behaviors were the primary focus of this work. For each activity a profile of activity vs. concentration was determined in order to identify a range of concentrations where the caged growth factor was inactive and the photolyzed factor was active with regards to cellular activity. In each case, the results using light-activated EGF (before and after photolysis) were compared to a commercial preparation of EGF or defined medium without growth factor or serum supplementation.

Initially, cellular activity in response to light-activated EGF was tested for assays performed in the controlled incubator environment. Though conditions in these assays were not identical to those in the instrument (e.g. closed system vs. open system, pH regulation by 5% CO_2 delivery to the surrounding environment vs. delivered to medium bottles prior to medium replacement, etc.), the advantage of many replicates and ability to test a range of concentrations in a single experiment outweighed the drawback of using the incubator environment as a model of the flow cell environment. Keeping this in mind,

the results of these assays provided a starting point to guide the selection of light-activated EGF concentration to test in the instrument.

2.1 Cell proliferation using light-activated EGF

One motivation for creating a light-activated growth factor was the potential to harness proliferation activity of cells using a soluble signal which could be controlled in time and space. The ability to achieve this would create a new method of cell patterning. Therefore, as a first step toward that goal, the activity of light-activated EGF before and after photolysis for stimulation of fibroblast proliferation was tested.

NIH 3T3 fibroblasts were maintained in Dulbecco's Modified Eagle Medium (DMEM) with 10 % Fetal Bovine Serum (FBS). Fibroblasts were harvested from monolayer culture with 0.25% trypsin/EDTA and collected via centrifugation. The following defined medium (free of serum and other mitogenic factors) was prepared: RPMI supplemented with 1X solutions of Serum Replacement 1 (Sigma, St. Louis) and SPIT (Sigma, St. Louis). The harvested cells were rinsed and centrifuged three times in the defined medium to wash away mitogenic factors before being plated into culture dishes.

To a culture of fibroblasts in defined medium, light-activated growth factor was added to obtain a final concentration of 50ng/ml. To a separate culture of fibroblasts, treated identically, light-activated EGF after complete photolysis (monitored by HPLC) was added. In control experiments, 50ng/ml of a commercially obtained sample of recombinant human EGF (positive control) or no growth factor (negative control) was added to the defined medium. The mean cell density in each culture as a function of time was determined by counting cells in twenty randomly chosen zones at regular intervals.

The result of the experiment to find proliferation of NIH 3T3 fibroblasts is shown in Figure 2. After photolysis, the unprotected synthetic growth factor stimulated

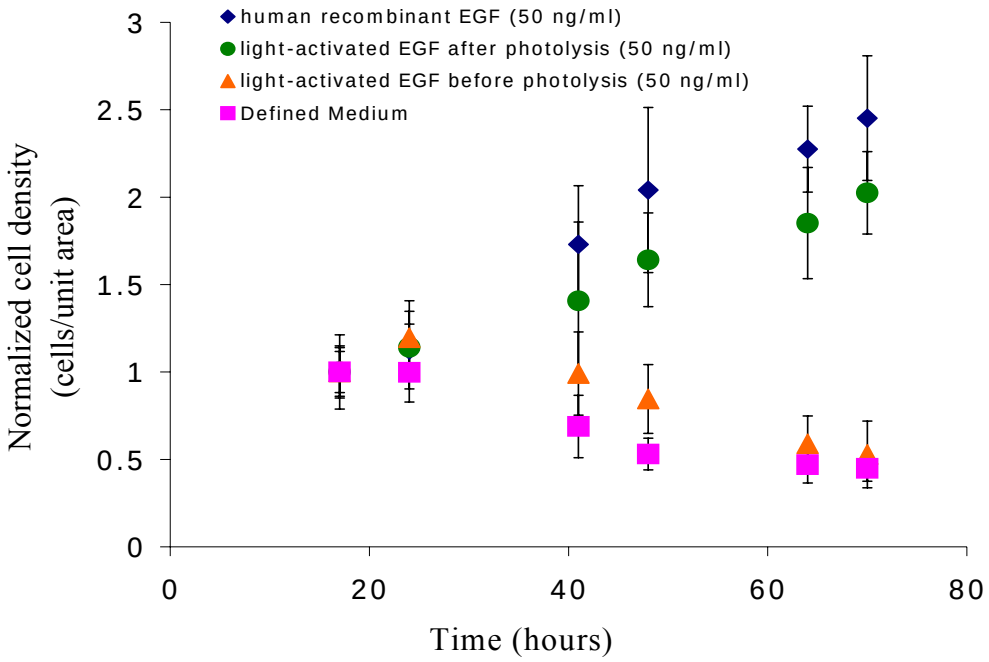

Figure 2. Proliferation if NIH/3T3 fibroblasts.

proliferation of fibroblasts to an extent similar to commercially obtained EGF. However, the protected growth factor did not stimulate proliferation at the concentration tested. In that case, the cell density (measured as a function of time determined by counting cells) slightly decreased to an extent similar to that in a factor free negative control.

The concentration dependence of the growth factor activity before and after photolysis was also determined. In this experiment, photolyzed and unphotolyzed factor (from the same stock) were added at varying dilutions to cultures of fibroblasts in defined

medium, which were then incubated for 36 hours prior to determination of the mean cell density.

The concentration dependence of the growth activity before and after photolysis is shown in Figure 3. At very high concentrations (>80 ng/ml) photolyzed and unphotolyzed growth factor had similar proliferative activities. However, over the concentration range of 25-50 ng/ml, the unphotolyzed growth factor displayed little to no activity, whereas the photolyzed growth factor displayed near maximal activity.

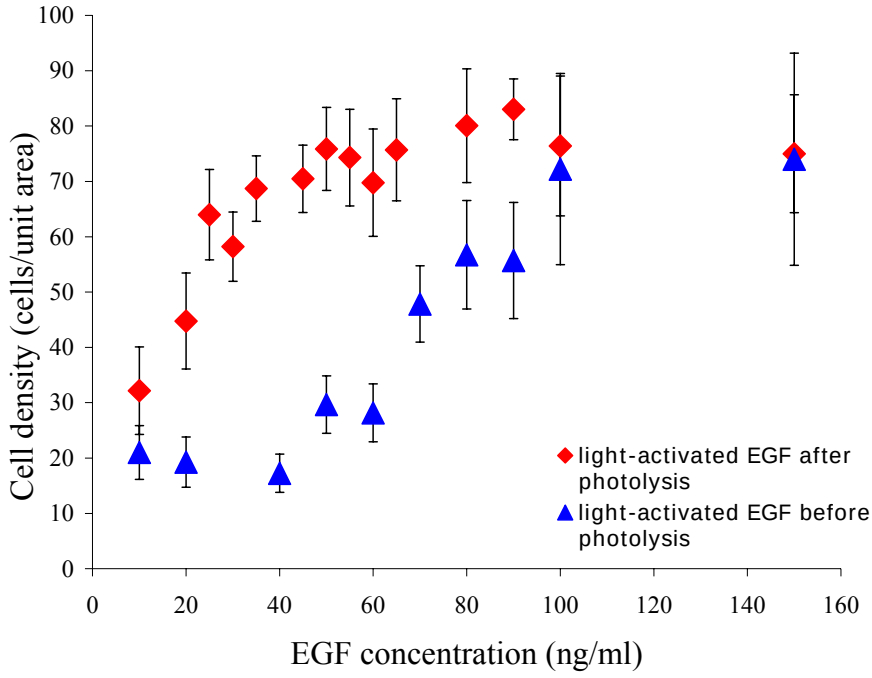

Figure 3 Concentration-dependence of EGF-stimulated proliferation of NIH/3T3 fibroblasts before and after photolysis. Error bars are 95% confidence intervals for means of multiple zones counted (n≥10).

These results demonstrated that rational protection of peptide residues with a photolabile group could produce a growth factor for which activity was not observed at

concentrations where photolysis yielded significant activity. Photolysis of the growth factor in a 50 ng/ml solution afforded conversion from little proliferative activity to near maximal activity. The non-linearity of that response enhanced the spatial resolution with which growth factor activity could be photolytically controlled.

2.2 Stimulating cell migration using light-activated EGF

A primary dermal fibroblast cell line was selected for the cell migration studies. This choice was made since subsequent passages and lots of the dermal fibroblast cell line exhibited a more consistent response to the medium supplemented with EGF than the immortalized 3T3 fibroblast line.

Two types of migration assays were used to test the activity of light-activated EGF (before and after photolysis) for stimulating fibroblast migration: the Boyden chamber method (Boyden 1962; Kim, Mohan et al. 1999) and the "scratch wound" assay. While the Boyden chamber method offered the unique advantage of distinguishing between chemotactic and chemokinetic migration, the "scratch wound" assay has closer resemblance to the migration in the flow cell environment (unrestricted movement across a surface instead of squeezing through a membrane).

2.21 Fibroblast migration response to human recombinant EGF using the Boyden chamber assay

The Boyden chamber method was used to measure dermal fibroblast migration toward a commercially available preparation of human recombinant EGF, synthetic light-activated EGF (before and after photolysis) and defined medium without growth factor. One advantage of this type of migration assay, due to the establishment of chemoattractant gradients, was that it provided a way to distinguish between chemotactic

and chemokinetic migration. The gradients in this assay are created between upper and lower chambers separated by a thin membrane containing pores. Cells are seeded into the upper chamber and can migrate toward the lower chamber by squeezing through the pores in the membrane. Migration is allowed to continue for a fixed period of time, after which cells are removed from the upper membrane surface with a cotton swab. Cells on the lower surface of the membrane are fixed with ethanol. The membrane is then removed from the chamber and stained with azure A, eosin Y, and methylene blue to enable counting of cells with a light microscope. Chemotactically migrating cells squeeze through the pores toward a positive chemoattractant gradient. Cells that are moving chemokinetically migrate in the absence of a gradient, but may increase their migration in the presence of higher concentrations of chemoattractant.

Experiments were carried out in order to establish basic parameters for the assay. Chemotactic migration was assessed for human dermal fibroblasts using a boyden transwell device. The upper and lower chambers of the device were separated by a collagen coated, polycarbonate membrane with 8 μm pores. Gradients were established by adding defined medium containing human recombinant EGF into the lower chamber and cells in defined medium

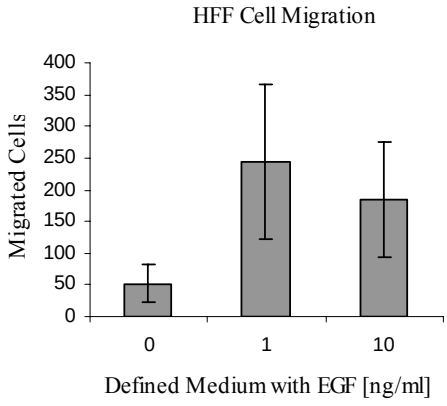

Figure 4 Fibroblast migration stimulated by EGF. Each value is the mean of six measurements. Error bars are the standard deviation.

(without growth factor) into the upper chamber. Migration conditions were tested for gradients established with 0-10 ng/ml EGF in the lower chamber, since that range was known to stimulate peak migration for a variety of cell types (Grant, Khaw et al. 1992; Ware, Wells et al. 1998; Polk and Tong 1999; Gorenne, Nakamoto et al. 2003). The cells were seeded into the upper chamber at a density of 5,000 cells/well and allowed to migrate over 4 hours. At this time, the migrated cells were assayed as described above. The migratory response was quantified as the number of cells counted on the lower surface of the membrane.

For an experiment with six replicates (n=6), there was 4.7 and 3.5 fold higher migration toward 1 ng/ml and 10 ng/ml EGF (respectively) than in wells containing only defined medium (no growth factor gradient), Figure 4. This response indicates that epidermal growth factor stimulates a migration response from dermal fibroblast cells.

2.22 Fibroblast migration response to light-activated EGF using the Boyden chamber assay

To determine the extent fibroblasts will migrate toward light-activated EGF (before and after photolysis), experiments were done to quantify the migratory response using the Boyden chamber. Basic parameters for the assay were maintained (i.e. number of cells, collagen coated membrane, migration time, etc.). The response of human dermal fibroblasts migrating toward light-activated EGF and light-activated EGF after photolysis was tested (n=5) for the following concentrations in defined medium: 1 ng/ml, 5 ng/ml, and 10 ng/ml. Controls were done in parallel with medium containing no growth factor or 1 ng/ml commercial EGF since this was the concentration which stimulated the greatest

migratory response in previous experiments. The result of this experiment is shown in Figure 5.

For concentrations above 1ng/ml, the migration response to caged and photolyzed EGF were within one standard deviation of each other. However, there was

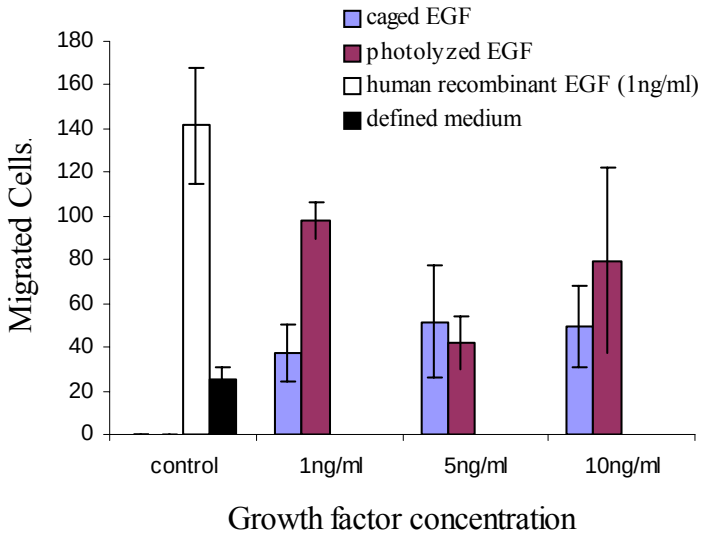

Figure 5 Fibroblast migration stimulated by different concentrations of caged and photolyzed EGF. Each value is the mean of five measurements. Error bars are the standard deviation.

more than a two-fold increase in migration toward photolyzed EGF compared to caged EGF at the 1ng/ml concentration. The response at this concentration indicated that photolysis activated the ability of the factor to stimulate cell movement. The number of cells migrating in response to the fully photolyzed EGF was close to the number of cells migrating in response to the same concentration of commercially obtained EGF. On the other hand, the number of cells migrating in the presence of the caged EGF was close to

the number of cells migrating in the absence of any growth factor, suggesting that masking glutamate 40 was effective at blocking the effects of EGF on cell migration.

2.23 Boyden checkerboard assay with human recombinant EGF

In checkerboard assays, an array is created by varying the concentrations of chemoattractant in both upper and lower chambers creating positive, negative or no gradient. The number of cells migrated is plotted in a checkerboard table to distinguish between cells migrating in the presence of an increasing gradient or no gradient. Cells that migrated in the absence of a gradient are positioned along the diagonal of the checkerboard chart, representing chemokinetic migration. A checkerboard assay for human dermal fibroblasts was performed with human recombinant EGF as the chemoattractant. Defined medium with either: 0, 0.2, 1 or 5 ng/ml EGF was added to 4 lower chambers in 4 rows. Human dermal fibroblast cells suspended in defined medium with either: 0, 0.2, 1 or 5 ng/ml EGF were added to 4 upper chambers in 4 columns at a density of 5,000 cells/well so that a 4x4 array was created. After 4 hours migration, the experiment was assayed as previously described.

The result of the checkerboard assay is shown in Figure 6. In the table, the top row is the concentration of EGF (ng/ml) in the upper chamber (with cells). The first column represents the concentration of EGF (ng/ml) in the lower chamber. The diagonal grey area shows migration in the presence of no gradient. In three experiments (n=2), both chemotactic and chemokinetic migration were observed. As seen along the diagonal grey area, the chemokinetic response increases with increasing concentration of EGF in the absence of a gradient, peaking at 1 ng/ml. The second column relates the chemotactic response observed for increasing concentrations of EGF, which also peaked at 1 ng/ml

EGF.

	0	**0.2**	**1**	**5**
0	0 +/- 0	0 +/- 0	16.5 +/- 21.9	0 +/- 0
0.2	20 +/- 17	25.5 +/- 30.4	52 +/- 73.5	6.5 +/- 3.5
1	132.5 +/- 12	136 +/- 15.6	236 +/- 56.6	45.5 +/- 58.7
5	62 +/- 56.6	141 +/- 46.7	86 +/- 31.1	61 +/- 62.2

Figure 6 Checkerboard assay of chemotactic and chemokinetic migration of fibroblast cells toward EGF. The top row is the concentration of EGF (ng/ml) in the upper chamber (with cells). The first column represents the concentration of EGF (ng/ml) in the lower chamber. The diagonal grey area shows migration in the presence of no gradient; EGF stimulates chemokinetic migration of HFF cells. Each value is the mean of two measurements and range.

2.24 Boyden checkerboard assay with light-activated EGF

In order to determine whether light-activated EGF after photolysis would also provoke a chemotactic response, a checkerboard assay for human dermal fibroblasts was also performed using light-activated EGF after photolysis as the chemoattractant. Defined medium with either: 0, 0.1, 1 or 5 ng/ml photolyzed EGF was added to 4 lower chambers in 4 rows. Human dermal fibroblast cells suspended in defined medium with either: 0, 0.1, 1 or 5 ng/ml EGF were added to 4 upper chambers in 4 columns at a density of 5,000 cells/well so that a 4x4 array was created. After 4 hours migration, the experiment was assayed as previously described.

The checkboard assay experiment was carried out in triplicate. The results are shown in Figure 7. Both chemotactic and chemokinetic migration were measured. In the figure, the top row is the concentration of photolyzed light-activated EGF (ng/ml) in the upper chamber (with cells). The first column represents the concentration of photolyzed

light-activated EGF (ng/ml) in the lower chamber. The diagonal grey area shows migration in the presence of no gradient, thus representing chemokinetic migration. The chemokinetic response increased with increasing concentration of photolyzed EGF in the absence of a gradient, peaking at 1 ng/ml. The chemotactic response was less apparent. The observed migration at the 1ng/ml concentration suggests that there is a chemotactic

	0	**0.1**	**1**	**5**
0	$26^{\pm 7.8}$	$48.7^{\pm 16.7}$	$38^{\pm 30.6}$	$36^{\pm 16.5}$
0.1	$61^{\pm 20.3}$	$77.7^{\pm 27.5}$	$72^{\pm 29.1}$	$91.3^{\pm 21.5}$
1	$70^{\pm 23.1}$	$74.7^{\pm 32.1}$	$80^{\pm 20}$	$72.7^{\pm 23.9}$
5	$39.3^{\pm 20.3}$	$63.7^{\pm 29.1}$	$75^{\pm 23.5}$	$33^{\pm 18.2}$

Figure 7: Checkerboard assay of chemotactic and chemokinetic migration of fibroblast cells toward photolyzed light-activated EGF. The top row is the concentration of photolyzed light-activated EGF (ng/ml) in the upper chamber (with cells). The first column represents the concentration of photolyzed light-activated EGF (ng/ml) in the lower chamber. The diagonal grey area shows migration in the presence of no gradient. Each value is the mean number of three measurements and standard deviation.

response. However, this is less apparent at other concentrations. While the results are suggestive of a chemotactic response, the migrations at most of the corresponding concentrations are not outside of the experimental uncertainty. This is not the case for the migration response for the 1ng/ml concentration, which was previously determined to be the concentration where the migration response was optimal. At this concentration, there is an indication that light-activated EGF after photolysis also stimulates both chemokinetic and chemotactic activity.

2.25 Measuring fibroblast migration using the "scratch wound" assay

In the "scratch wound" assay, a culture of fibroblasts was grown to near confluence in DMEM supplemented with 10% FBS in 24 well culture plates. At this point, the medium was aspirated and replaced with serum-free defined medium then

incubated overnight. Cells were scraped off half of the surface of each well to create a cell-free region. The cultures were washed twice with serum-free defined medium and replaced with medium containing either no growth factor, recombinant human EGF, caged EGF or caged EGF after complete photolysis. The experiment was carried out in triplicate for the following growth factor concentrations: 0.01ng/ml, 0.05 ng/ml, 0.1 ng/ml, 0.5 ng/ml, 1 ng/ml, 5 ng/ml and 10 ng/ml. Cell movement was then measured over time as the cells migrated to fill in the scratch by counting the number of cells that migrated past 300μm into the cell-free region.

The difference between the numbers of cells that migrated in response to light-activated EGF after photolysis compared to light-activated EGF before photolysis increased with concentration, peaking at 1ng/ml. The same trend was observed for the migration ratios of human recombinant EGF to defined medium. At concentrations above 1ng/ml, both the number of cells that migrated and the difference between active and inactive EGF began to decrease. Once again, this was also the case for control experiments using native EGF or defined medium. The result is shown in Figure 8.

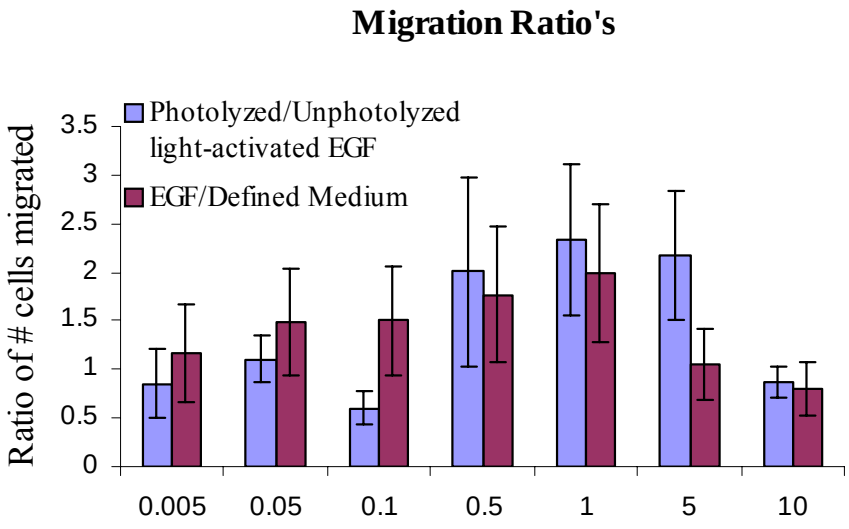

Figure 8: Scratch Wound Assay: concentration profile. Each value is a ratio of the means of three measurements. Error bars represent standard error of the ratio.

2.3 Summary of results

It was determined that after photolysis, concentrations over the range of 25-50ng/ml stimulated proliferation of fibroblasts. In fact, at 50ng/ml fibroblast proliferation was stimulated to an extent similar to commercially obtained human recombinant EGF at the same concentration. On the other hand, caged EGF over the same range of concentrations displayed little to no activity to an extent similar to that of defined medium, free of growth factors or mitogenic agens. These results indicate that it is possible to synthesize a caged growth factor for which little to no proliferation is observed at concentrations where photolysis releases its ability to have maximal activity. Therefore, there is a clear rational for testing the ability of light-activated EGF to spatially affect proliferation activity of fibroblasts.

The ability to affect fibroblast migration using light-activated EGF was also examined. The greatest migration response was observed for 1ng/ml concentrations of light-activated EGF. Subsequently, this was also the concentration for which commercially obtained human recombinant EGF also stimulated maximal migration. The migration response to caged EGF at 1ng/ml was within the experimental uncertainty of fibroblast migration in defined medium without growth factor. The distinction between a chemokinetic and chemotactic migration response to light-activated EGF, measured with the Boyden checkerboard assay, was less apparent. However, the indication that 1ng/ml light-activated EGF (after photolysis) did stimulate both chemotactic and chemokinetic activity was enough motivation to test the effects of spatially resolved photolysis on fibroblast migration.

2.4 Materials and Methods

General Cell Culture

NIH 3T3 fibroblasts (ATCC, CRL-1658) were maintained in Dulbecco's Modified Eagle Medium (DMEM; Gibco, Frederick, MD) with 10 % Fetal Bovine Serum (Sigma, St. Louis, MO). Fibroblasts were harvested from monolayer culture with 0.25% trypsin/EDTA (Gibco, Frederick, MD) and collected via centrifugation.

Human Foreskin Fibroblast (HFF; CRL 2522) cells were maintained in Dulbecco's Modified Eagle Medium (DMEM; Gibco, Frederick, MD) with 10 % Fetal Bovine Serum (FBS; Sigma, St. Louis, MO). Prior to reaching confluence, the fibroblasts were harvested from monolayer culture with 0.25% trypsin/EDTA (Sigma, St. Louis, MO). Trypsin was neutralized with 10% FBS in DMEM. Fibroblasts were harvested for experimentation until the 9^{th} passage (approximately 25 doublings). The ATCC product specification for this cell line states a proliferation capacity for 52 population doublings before the onset of senescence.

Preparation of Defined Medium

The following defined medium (free of serum and other mitogenic factors) was prepared: RPMI Medium 1640 (Gibco, Frederick, MD) supplemented with L-glutamine, 1x solution of Serum Replacement 1 (Sigma, St. Louis, MO) and 5ng/ml Sodium Selenite, 0.12mg/ml Pyruvate, 0.01mg/ml Insulin from bovine pancreas, and 5.5µg/ml Transferrin (SPIT medium supplement) (Sigma, St. Louis, MO). When indicated, commercial preparations of human recombinant EGF were obtained from Sigma (St. Louis, MO).

Photolysis of Light-Activated EGF

Stock solutions of light-activated EGF (25μg/ml) dissolved in equal volumes of Acetonitrile and milli-Q water containing 0.05%TFA were prepared. Photolysis of the stock solution took place in a quartz cuvette at 365nm irradiation, 30mW/cm^2, for 30min. The photolysis protocol was established based on an analysis of the rate of photolysis to fully remove the caged compound from the light-activated EGF under these conditions.

Boyden Chamber Assay

Corning 24-well Transwell plates with upper and lower chambers separated by polycarbonate membranes with 8 μm pores were obtained (Corning, Lowell, MA). A 3mg/ml solution of collagen dissolved in 0.12N HCl was added to an equal volume of 70% ethanol and mixed by vortex. To each membrane 35μl of the collagen-ethanol solution was added and allowed to dry for 2h in a sterile laminar flow hood.

In the boyden assay, gradients were established by adding 600μl of defined medium containing various concentrations (indicated in the text) of commercial preparations of human recombinant EGF, light-activated EGF (before and after photolysis) or no growth factor. To the upper well, 100μl of an HFF cell suspension ($5x10^4$ cells/ml) in defined medium (either with or without growth factor, concentrations indicated in the text) was added and allowed to migrate over 4 hours in a humidified incubator. At this point, cells were removed from the upper membrane surface with a moistened cotton swab. Each membrane was rinsed in a 1x solution of PBS and then the cells remaining on the lower surface were fixed with 70% ethanol. The membrane was removed from the chamber and stained with azure A, eosin Y and methylene blue to enable counting of cells with a light microscope.

“Scratch Wound” Assay

A culture of HFF fibroblasts were grown to near confluence in DMEM supplemented with 10% FBS in 24 well polystyrene culture plates. At this point, the medium was aspirated and the wells were washed twice with 2ml of defined medium. After the final wash, the culture was subjected to an overnight serum starvation in defined medium. Cells were scraped off half of the surface of each well, using a pipette tip, to create a cell-free region. The cultures were washed twice with defined medium. The medium was replaced with defined medium containing either no growth factor, recombinant human EGF, caged EGF or caged EGF after complete photolysis. The experiment was carried out in triplicate for the following growth factor concentrations: 0.01ng/ml, 0.05ng/ml, 0.1ng/ml, 0.5ng/ml, 1ng/ml, 5ng/ml and 10ng/ml. Digital microphotographs were taken of the scratch border at the 0h and 36h time point. The images were compiled using Adobe® Photoshop® Photomerge function and then superimposed. The number of cells that migrated past 300μm into the cell-free region was counted for each concentration and replicate.

CHAPTER THREE

DESIGN OF THE INSTRUMENT

3.0 Design Parameters

The greatest benefit of controlling cell behavior with a soluble, light-activated growth factor is that its activation can be controlled; signaling of cell behavior is not constrained to a single activation pattern. This means signals can be created and controlled with greater complexity in space and time than is typically available in vitro. Thus, the inherent advantage that an automated instrument adds to the technology is the precise timing, delivery and activation of the caged growth factor.

The instrument was designed to incorporate the following parameters: 1. The ability to create high resolution photo-activation patterns with complete automation that allowed timed delivery and removal of growth factors. 2. Refrigerated storage of medium containing caged growth factors. 3. Provide even heat distribution of the culture chamber at 37°C. 4. The ability to remove and replace the chamber at various times during an experiment for analysis while maintaining a closed sterile environment throughout the process. 5. Accurate realignment of the chamber upon replacement. 6. Management of media flow rates to ensure sheer stresses remain at biocompatible levels. 7. Integration of the light projection component with a device that allows interchangeable patterns which could be focused onto the flow chamber with cellular size resolution to allow for spatially controlled removal of the photolabile group from the light-activated growth factor.

To meet these parameters, the instrument consisted of five subsystems: the digital projection system, the electrical control system, the fluidics system, the flow cell

chamber, and the software. The design of this device was partially based on a previously built machine that integrated a digital micromirror device (DMD) with a computerized system for the automated fabrication of oligonucleotide arrays (Luebke 2002). Optical components, software framework, and electrical subsystem were essentially the same in both instruments.

The addition of tissue culture to the instrument required that several other components be changed to meet those demands. In the oligonucleotide array instrument, chemicals were pushed through a reaction chamber using pressurized gas. Inability to control fluid flow rate would wreak havoc on a tissue culture system. High fluid flow rates would create stress on the cell culture, disrupting its development. Therefore, to control the flow rate, the medium was drawn from its bottle by a peristaltic pump and delivered to the flow cell chamber. Culture medium must be refrigerated and equilibrated with 5% CO_2, while the culture itself is warmed to 37°C – which necessitated creating thermostatic control and a way of delivering gas to equilibrate the medium. The flow cell chamber was machined from biocompatible materials, and included windows to allow microscopic analysis during

Figure 9: A. Photograph of Instrument **B**. Automation of each component of the instrument is accomplished with computer control programming. **C**. Enlarged view of heated tissue flow chamber and illuminated DMD used to project images into the flow chamber.

the course of an experiment. Another difference between the oligonucleotide instrument and the tissue culture instrument was that the DMD model was an updated version, and thus interfaced to the control software differently from the version used in the oligonucleotide array instrument. Therefore, while the skeleton framework of the software remained the same, new programming routines integrated additional components into the tissue engineering system that the oligonucleotide array instrument did not contain. A photograph of the instrument is seen in Figure 9 and a detailed description follows.

3.1 The Digital Projection System

The digital projection system was designed to pattern images onto the culture chamber using light reflected from a digital light processing device projected, without magnification or reduction, with a custom six-lens element.

Patterns of light were projected onto the flow chamber with a Digital Micromirror Device (DMD) developed by Texas Instruments. The DMD was a matrix arrangement of 1024 x 768, 16 μm square mirrors spaced 1 μm apart. Each mirror could be independently controlled to project light toward or away from the culture chamber. The DMD was uniformly illuminated with a light source from a commercial vendor (Hamamatsu Corp., New Jersey). The light source was a LighteningCure UV Spot Light Source (L8333-01) equipped with an ozone-free, 200W Mercury-Xenon arc lamp (L8251), with an intense emission at 365nm. The lamp was equipped with a shutter to control illumination to the DMD to times when photolysis was

Figure 10: Close up of DMD

desired, preventing undesired photolysis by scattered light. The light source had a 15 pin D-sub type connector that allowed it to be controlled by an external device. The lamp was turned on by connecting pin 11 (lamp on trigger) to 15 (ground) on this connector. To turn the lamp off, pins 10 (lamp off trigger) and 15 were connected. The internal shutter of the lamp was opened by connecting pin 13 to pin 15, and closed upon disconnection. The relays described in the electrical control section controlled the connection of these pins.

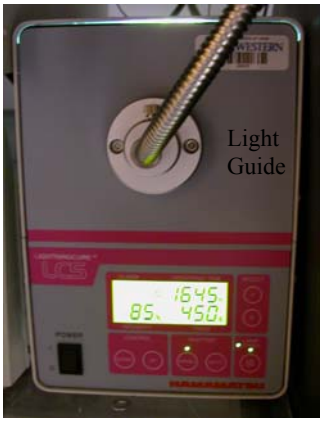

Figure 11: Hamamatsu UV Spot Light Source.

A quartz fiber optic light guide (A2873) was used to direct the light from the lamp to the lens system of the instrument. Brilliant Technologies (Denton, TX) developed a silica lens system to collimate the light beam. The light traveled from the light guide through a quartz integration rod, which provided light in the same aspect ratio as the DMD, followed by a magnifying lens. After this lens, the light passed through a 365 nm interference filter (Edmond Scientific, part # NT43-103) with a transmission peak width at half maximal of 2 nm. Other wavelengths were removed using a UV reflector (Edmond Scientific, part # 43454) which reflected in the 350-450 nm range at 45° and transmitted higher wavelengths. (Wavelengths below 365 nm were removed to prevent light induced damage to cells and other biological factors). The light reflected from the UV reflector to a conical mirror which directed it to the DMD. The light beam was reflected to the DMD at an angle of 20° off normal, resulting

in a reflected beam that was normal to the plane of the projection lens. From there, the patterns were reflected off a front surface mirror which directed it to the flow cell.

With this system, variation in light intensity across the projected image was less than 15%. The incident light power at 365 nm was 30 mW/cm^2 for a lifetime of 3000 hours. Improvements were made to the optical system after the development of the photolysis regimen to reach that power. At the time of development, the light power at the chamber was 12 mW/cm^2. An internal feature of the lamp offered the ability to reduce power output. So, in order to sustain reproducibility for future experiments, that intensity was maintained by lowering the power with that feature.

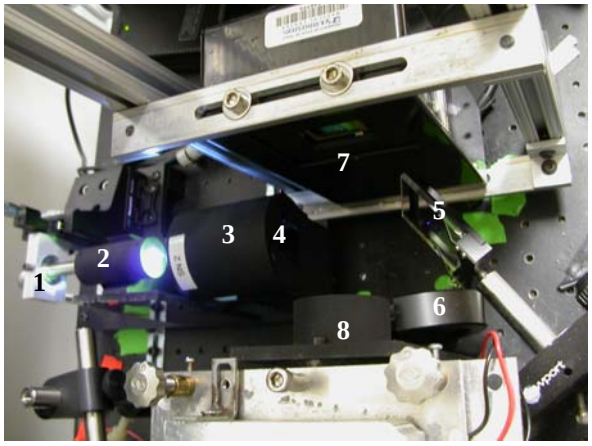

Figure 12: Lens System. 1.Light Guide 2.Integration Rod 3.Magnifying Lens 4.Interference Filter 5.UV Reflector 6.Conical Mirror 7.DMD 8.Projection Lens.

3.2 Electrical Control System

The instrument electrical control system was responsible for the simultaneous operation of multiple devices. Essentially, this system was responsible for mediating software commands to hardware activity, enabling automation and coordination of the devices.

3.21 System Automation

The technology of controlling cellular behavior using photo-caged moieties would require precise timing of the delivery and activation of the caged growth factor. In addition, an advantage of controlling cell behavior with a light-activated soluble signal is the benefit of not being constrained to a single activation pattern. As the culture progresses, timing and delivery of the signal can be adjusted to meet changing demands. Since it would be impractical for an operator to be present for the entire process, an automated device was necessary in order to take full advantage of the unique features offered by the technology.

3.22 Multiple Input Devices

Even though most of the components between the oligonucleotide instrument and the one described here were different, the criterion that multiple input devices were required (i.e. light source, solenoid valves, peristaltic pump, and DLP), mandated the decision to include an identical I/O control, signal conditioning and relay system.

3.23 Final Electrical System Design

A single computer controlled the input devices to coordinate their activity. The computer could direct the operation of 16 solenoid valves, the DMD, turning on and off of the mercury-xenon lamp, as well as control of its shutter, the peristaltic pump, flow cell temperature measurement and thermostatic control of the heated stage where the flow cell rested. The system was designed to allow simultaneous operation of each of those activities. However, images were only projected after the flow of medium into the flow cell had ceased and time had been allowed for any turbulence (which could disrupt patterning) to settle.

The DMD and pump input directly to the computer via USB and DB-15 pin connector, respectively. However, the solenoid valves, lamp, heater and thermocouple interfaced via two multifunction input/output (I/O) devices (National Instruments, part # PCI-1200). The I/O device that controlled the solenoid valves and lamp was connected to an adaptor board (National Instruments, part # SC-2053) which in turn connected to two digital signal conditioning boards (National Instruments, part # SC-2062). Each digital signal conditioning board had eight electromechanical relays which were used to control the solenoid valves of the fluidic system and lamp functions. The relays had a normally open, normally closed and common contact. Electrical connections were made to the normally open (N.O.) and common (COM) contacts of the relays. A 12 VDC potential activated the solenoid valves, however each relay was certified to withstand operation up to 6A at 30VDC. The relays were connected in parallel to a 12 VDC power source (an AC/DC power converter converted a 120 VAC signal from a standard wall outlet to a 12 VDC signal). For the scope of this work, no more than 4 valves operated simultaneously,

however the system could withstand simultaneous operation up to 12 valves.

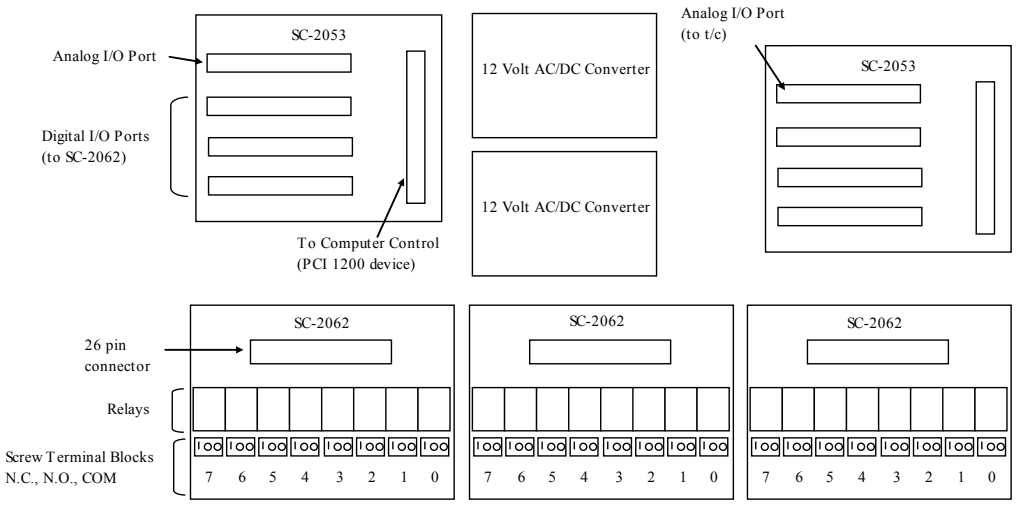

Figure 13: Schematic representation of the electrical control box. The schematic shows the two cable adaptor boards (SC-2053), the AC/DC power converters, and the digital signal conditioning boards (SC-2062).

The I/O device that controlled the flow cell stage heaters and thermostat also interfaced with an adaptor board. The analog input of the adaptor board connected to a thermocouple which sensed the internal temperature of the flow cell. The digital input of the adaptor board was connected to a digital signal conditioning board with eight electromechanical relays. One electromechanical relay on this board served as an on/off power switch to regulate the heaters of the mounting stage where the flow cell rested. Operation of this switch was controlled through a software program which used input from the thermocouple to regulate temperature within a +/- 1°C limit. Figure 13 shows the schematic representation of the components inside the electrical control box.

The computer was an Intel Pentium Optiplex GX400 1.7 GHz with 523 MB of RAM, a 74.5 GB hard drive and a Microsoft Windows 2000 operating system. The

multifunction I/O devices had 24 digital I/O lines and interfaced to the computer through PCI slots. Two 50-pin ribbon cables (National Instruments part # 180524-20) connected the multifunction I/O cards to the adapter boards (National Instruments part # SC-2053). A 5V DC signal was necessary to power each digital signal conditioning board. An AC/DC power converter converted a 120VAC signal to the required 5V DC signal. A backup power supply (APC, part # RS 1500) was used to prevent temporary surges or power outages in the building's power supply from causing an unplanned termination during the course of an experiment. The computer, DMD, lamp and pump were connected to the power supply. The power supply was rated to handle 865W/1500 VA load for 20.5 minutes.

3.3 Fluidics System

The instrument was equipped with a compact refrigerator (Kenmore, 564.91245100) to store and maintain the medium at 20°C. Holes were drilled through the wall of the refrigerator for the media and 5% CO_2 lines to be threaded through. The medium was delivered to the culture chamber using a digitally controlled peristaltic pump (Masterflex, part # 7550-10). The peristaltic pump allowed for a high level of control over the rate of fluid delivery to the chamber. The pump was positioned downstream of the chamber and fluid was drawn through the system, gated by a series of computer controlled, electronically actuated solenoid valves. The valves were normally closed either 2-way (Cole Parmer, part # A-01367-70) or 3-way (Cole Parmer, part # A-01367-72) 12 VDC, 15 PSI Teflon™

Figure 14: Masterflex Peristaltic Pump.

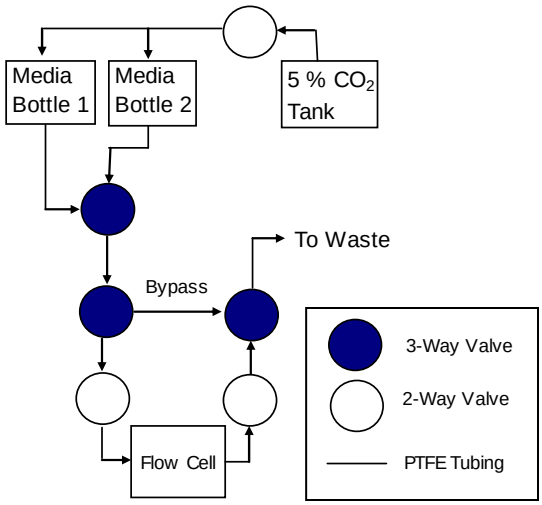

Figure 15: Schematic drawing of fluidic valve system.

valves. Polytetrafluoroethylene (PTFE) tubing with 1/16" outside diameter, 1/32" inside diameter was used for the fluid lines. Waste was emptied into a 2L flask positioned downstream of both the flow cell and pump. A schematic drawing of the valve fluidic delivery system is shown in Figure15.

One line of tubing into the refrigerator was reserved for delivering 5% CO_2 to each bottle of media using a Teflon™ manifold (Upchurch Scientific, part # P632). The gas was delivered to each bottle at regular intervals, gated by one solenoid valve. Each bottle of medium had three tubes feeding into it, one for fluid delivery, one for 5% CO_2 delivery and one to vent. The gas line and vent each had a 0.2 μm syringe filter (Nalgene, part # 194-2520) to prevent bacteria and fungal contamination in the medium.

3.31 Tissue Culture Flow Cell

The tissue culture was housed within a closed parallel plate flow chamber with transparent windows on opposite sides (Figure16). The inlet and outlet port was sealed with a rubber septum (EPS, Inc., part # IV2004) which was punctured by 22 gauge syringe needles in line with the tubing of the fluidic system. Only biocompatible materials came in contact with the culture. The main body of the chamber was milled

from Teflon™ with embedded silicone rubber o-rings to create a seal between the body and the chamber windows, one of which supported the cell culture. Silicone o-rings (Marco Rubber & Plastic Products, Inc., part # S1000-016) were specifically chosen for seals in the flow cell since silicone does not support the growth of bacteria.

The internal wall of the chamber, where the cell culture resides, was designed with circular shaped walls. This geometry was important because of the influence the sidewall of the chamber has on fluid flow. The radial geometry provided the most uniform flow, since there would be no corners to introduce turbulence as the medium is exchanged.

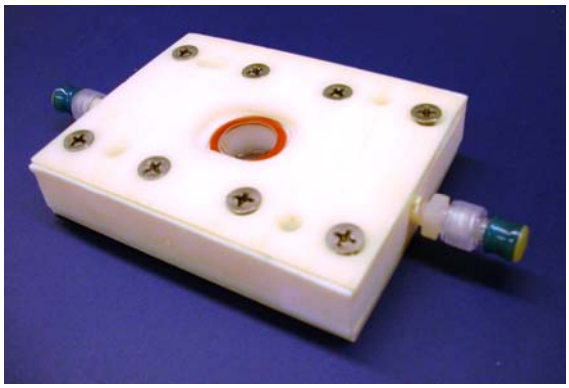

Figure 16: Photograph of Flow Cell Chamber

Parallel-plate flow cell chambers, such as the one described here, promote even distribution of cell growth by preventing uneven growth factor concentration gradients caused by entrapment from sidewall effects (Peng 1996).

Glass slides provided the transparent window for light activation and a convenient means for microscopic analysis during the course of an experiment. The chamber rested on an aluminum stage which could be adjusted with micrometer precision in the x-y-z positions to ensure the highest degree of focused image in the desired plane. Mounting pins on the aluminum stage ensured exact placement of the chamber.

3.4 Flow Cell Temperature Control

A heated aluminum cover rested on top of the mounted chamber to provide even heating. The aluminum stage and cover were heated with Kapton etched foil resistive heaters (Watlow, part # K05711980A) and regulated thermostatically. Both the stage and cover were machined from aluminum, which distributes heat evenly. The heaters were wired in parallel so that the total resistance for these heaters was 44.2 Ω. The heaters were powered by a variable source power supply (Elenco Precision, XP-581) set at 9VDC. A relay inline with the power supply turned the heaters on and off. Switching of this relay was controlled by a software program.

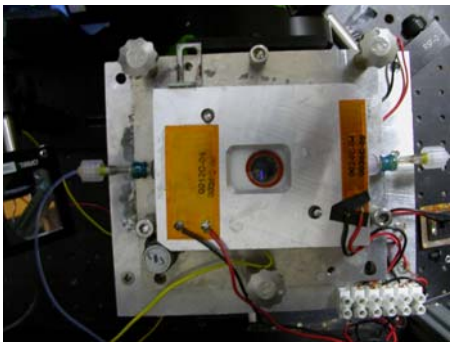

Figure 17: The flow cell stage with cover is heated with Kapton etched foil heaters which are thermostatically controlled by a program that uses temperature readings from a type K thermocouple (yellow wire in photo), housed in a port on the side of the chamber, to control power to the heaters.

3.5 Temperature Control Software

Due to interference between data acquisition boards, it was necessary to use separate control software for the thermostat. National Instruments Labview software contains functions to convert and display thermocouple readings into graphic

Figure 18: Temperature Control Display. A scrolling chart (purple) displays real-time temperature readings taken from the thermocouple housed in the flow cell.

temperature readouts in real-time. Therefore, this program was selected for the thermostat control software. The purpose of this program was to use temperature information to regulate power to the flow cell stage heaters. The software program received temperature input from a type K thermocouple housed in a port in the side of the flow cell. The program took the average of five readings from the thermocouple for the graphic temperature display. The temperature set point for the program maintained the temperature at 37°C +/- 1°C.

3.6 Control Software

The software package for the instrument acted as the user interface that accepted instructions to control operations of the various components. This software was a custom design modified from Visual Basic code originally written for the oligonucleotide array system (Luebke 2002). New programming routines were necessary in order to integrate additional components (i.e. pump, updated DMD, 5% CO_2, etc.) into the device that the oligonucleotide instrument did not contain.

The code parsed instructions from ‘macro’, ‘scheme’ and ‘ohf’ text files. The ‘macro’ text file contained the instructions and parameters to call up subroutines which controlled the components of the instrument; relays, valves, peristaltic pump, lamp, and DMD. The macro file was made up of three sections; each separated by a row of asterisks. The first segment provided the scheme file pathway. The second segment was the main body of the control commands entered by the user. It contained command instructions for one cycle of an experiment. Typically, one cycle was the period for the illumination regimen until medium replacement. The third section was reserved for any

shut down procedures, such as turning off the lamp. The number of cycles for the program was set by the user in the *.ohf text file.

The ‘scheme’ file was a text file that matched a given name to a specific relay. The scheme file was designed into the programming to simplify the information a user had to enter to run an experiment, therefore minimizing operation errors. The program used information from the ‘scheme’ and ‘macro’ files in subroutines that carried out specific events, such as, directing medium into or around the flow cell.

The *.ohf file provided timing information to the software control program. This file contained instructions for the number of cycles the body of the macro command file would be run and the time interval for the release of 5% CO_2 into the media bottles. Note: a timing function in the control software automatically triggered the release of CO_2 independent of other command functions being carried out.

User created bitmap image files contain the DMD digital mask pattern information, sized (1024x768) so that one mirror was represented by one pixel. One bitmap file was used for each pattern.

3.61 Instrument control software macro script language

The script language was constructed to simplify experimental design for new users. With the aid of the script language, made up of ten commands, it was not necessary for the user to have extensive programming knowledge to run the software. The command lines were:

Use Scheme: (followed by the file location)

Include (followed by the file location)

Image (followed by file location)

Open Shutter for (a variable integer) millisecond(s)

Wait (a variable integer) millisecond(s)

For (a variable integer) millisecond(s), release '(media bottle name)', (around or into) flow cell

Pump (a variable integer) milliliter(s) at (flow rate) ml/min

Lamp ON

Lamp OFF

In the above list of commands, 'a variable integer' represents the duration time in millisecond(s), 'media bottle name' is the name of the bottle of media as defined in the scheme file, and 'flow rate' is the rate of speed that the pump draws the fluid either into or shunted around the flow cell. The flow rate was always programmed for 0.5 ml/min for the work represented in this document.

CHAPTER FOUR

CHARACTERIZATION OF INSTRUMENT

4.0 Characterization Parameters

The instrument was designed to incorporate a number of parameters to enable investigations using highly resolved activation of light activated growth factors to control cell behavior. Characterizing the operation of the instrument was critical in developing a protocol for controlling cell behavior using light-activated EGF. The instrument was specifically tested for its ability to: create high resolution patterns of photolysis, realign the flow cell upon removal and replacement (without disrupting the photolysis pattern), determine conditions for maintenance of cell culture (medium replacement, pH, flow rate, temperature, and the prevention of fungal or bacterial contamination).

Assays were developed to test the function of each sub-system. The optical subsystem of the instrument was characterized using surface photochemistry techniques to examine the resolution with which photolysis patterns could be created and maintained upon removal and replacement of the chamber. The tissue culture sub-system was tested to determine how long and under what conditions cell culture could be maintained. Specific attention was paid to identifying the frequency with which medium had to be replaced to sustain vitality of the cell population, rate of flow at which medium could be replaced without disrupting cell attachment or movement, and conditions and procedures that prevent fungal or bacterial contamination.

4.1 Digital Projection System

To analyze the resolution of the optical components, test images were projected from the DMD onto a glass slide covalently coated with a photoreactive group

(MeNPOC-thymidine). Photolysis of this group with 365 nm light generates a hydroxyl that can be probed by coupling with a flourophore-labeled (Cy3) phosphoramidite. A fluorescent image of the 365 nm light projected onto the glass slide was thus generated and visualized with a fluorescence scanner, Figure19.

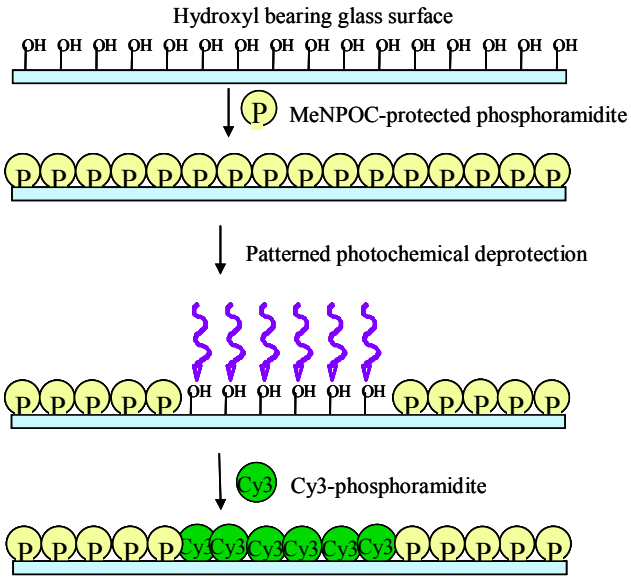

Figure 19: Schematic of the assay used to focus the instrument.

This method was used to adjust the top surface of the lower window glass slide into the focal plane of the DMD projection. Single mirror (16μm x 16μm) resolution was achieved using this technique (Figure 20). This method was also used for locating variations in the light intensity due to shadows caused from misalignment of the optical components. While quick measurements of the light power intensity can be made using a UV photometer, measurements using photochemistry provided photolysis information about the entire projection area. This was done by projecting images of rectangular strips of light for increasing amounts of time. Then plots of the ratio of image intensity to

background against time were made to determine the photolysis half-life, from which the power flux could be directly calculated (McGall 1997).

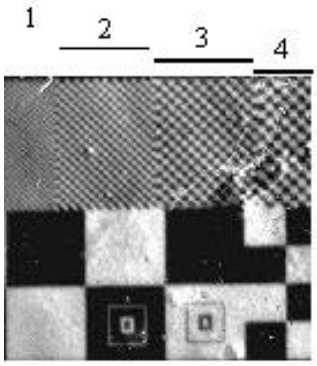

Figure 20: Fluorescent image patterned by projection onto glass surface coated with a photoreactive group. Image was created as described in the text. The squares in the checkerboard patterns in the top half of the image are **1**: 34µm, **2**: 51 µm, **3**: 68 µm, and **4**: 85 µm. The concentric square outlines in the bottom half of the image are made with 16 µm lines (outer square) and 34 µm lines (inner square). Bright spots are due to an artifact of washing the fluorescent stain during imaging.

The reproducibility with which the flow chamber could be replaced after removal was also tested using the same surface photochemistry method. Images of arrows with different orientations were projected onto the photoreactive surface. The chamber was removed and replaced and another set of arrows, mirror reflections of the first set, were projected (Figure 21). The projected images were visualized, and the x-y variation in repositioning the chamber was then determined. The experiment was repeated six times.

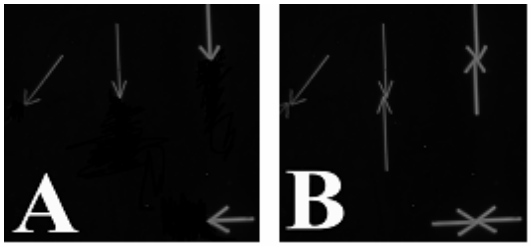

Figure 21: Chamber positioning. **A**. First set of images projected onto chamber. **B**. Addition of second (mirror) image projected after removal and replacement of chamber.

The average variation was 4 pixels (64 µm) along the x-axis and 2.5 pixels (40 µm) along the y-axis. This variation represented the limit of the spatial precision with

which photolysis patterns could be maintained. It corresponded to the tolerance or precision with which the locating pin-hole placement could be machined during manufacturing of the flow cell and stage. For the purpose of this work, this variation did not interfere with the effectiveness of the system. In fact, it was only slightly larger than one human dermal fibroblast cell size.

4.2 Establishing Culture Parameters of the Flow System

Since CO_2 was delivered to the media bottles and not directly to the flow chamber, the medium needed to be replaced frequently to maintain appropriate pH. A culture of NIH/3T3 fibroblasts was seeded evenly into the flow cell in DMEM supplemented with penicillin-streptomycin and 10% Fetal Bovine Serum. The chamber was placed in an incubator at 37°C until the cells adhered and spread onto the glass surface of the chamber. The chamber was then placed onto the instrument and the medium was replaced at regular intervals. The chamber was removed daily and observed by light microscope with phase contrast. This experiment was repeated for 1-24h frequencies of medium replacement until a frequency at which cells continued to proliferate was identified (as monitored by averaging 5 random zones of cell density). It was necessary to replace the medium in the chamber every 4 hours or less.

In addition, medium replacement flow rates (from 0.5ml/min to 10 ml/min) were tested. It was determined that flow rates above 2 ml/min caused fibroblasts to detach from the glass window. Flow rates at or below 2 ml/min did not appear to have an effect on the cell cultures. Initial experiments were carried out at 2ml/min, however, the lower rate limit of the peristaltic pump was 0.5 ml/min. Thus, this rate was ultimately chosen as the experimental standard since it was below what was observed to cause disruptions due

to hydrodynamic forces on the cell culture. Fibroblast cultures were maintained for weeks at this medium replacement frequency and flow rate.

4.21 Maintaining cell culture with EGF: Intermittent exposure

Once the basic fluidic system parameters of maintaining cell cultures in the instrument were established, experiments were carried out to establish the EGF exposure required by cells. While it has been reported that cells do not require continuous growth factor exposure to proliferate (Jones and Kazlauskas 2001), it has not been reported what frequency and duration of EGF exposure is required to sustain activity. This is important in our system because as caged EGF becomes activated by photolysis, it will begin to diffuse; thereby depleting the concentration of active EGF available to cells below what is necessary for signaling. It is not desirable to irradiate constantly since constant diffusion of active EGF would reduce the spatial resolution of the signal. Additionally, constant exposure of UV irradiation is damaging to cells and so is not possible.

Therefore, the instrument was used to study the temporal requirements of EGF exposure to fibroblasts required to stimulate proliferation under serum-free conditions. This was done by delivering 6 ml of defined medium with EGF (50 ng/ml) over 3 minutes to a culture of fibroblasts in the flow chamber, allowing the factor to remain in the chamber for 10 minutes before flushing it away with 6 ml defined, growth factor free medium at a 2ml/min flow rate. The defined medium was left in the chamber for 30 minutes and then the procedure was repeated continuously throughout the experiment. At various times, ten randomly selected fields were counted visualizing phase contrast light microscopy.

Proliferation of the cells in the intermittent EGF exposure experiment is shown in Figure 22, represented by diamonds. This protocol resulted in a proliferation doubling time of 45 hours.

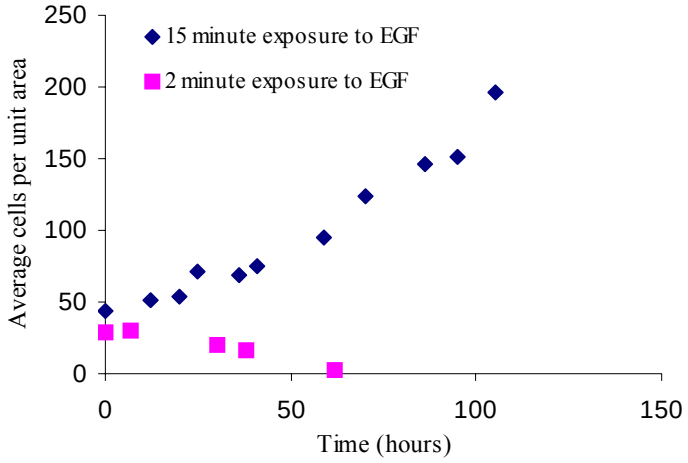

Figure 22: Proliferation of fibroblasts with intermittent exposure to EGF.

To ensure that proliferation was not due to continuous traces of growth factor left behind after the wash, a control experiment was performed. In this experiment, 4ml defined medium containing EGF (50 ng/ml) was introduced over 2 minutes, and immediately washed away with 6ml defined medium delivered at a 2ml/min flow rate, followed by a 30 minute period in defined, growth factor free medium. Continuous repetition of the protocol where the EGF was immediately washed away did not promote proliferation of the fibroblasts (Figure 22, squares). This outcome indicated that proliferation was not due to continuous exposure of traces of growth factor left behind after the wash, but to the intermittent exposure to EGF for 15 minutes out of every 45 minute period.

4.3 Materials and Methods

General Cell Culture

NIH 3T3 fibroblasts (ATCC, CRL-1658) were maintained in Dulbecco's Modified Eagle Medium (DMEM; Gibco, Frederick, MD) with 10 % Fetal Bovine Serum (Sigma, St. Louis, MO). Fibroblasts were harvested from monolayer culture with 0.25% trypsin/EDTA (Gibco, Frederick, MD) and collected via centrifugation.

Human Foreskin Fibroblast (HFF; CRL 2522) cells were maintained in Dulbecco's Modified Eagle Medium (DMEM; Gibco, Frederick, MD) with 10 % Fetal Bovine Serum (FBS; Sigma, St. Louis, MO). Prior to reaching confluence, the fibroblasts were harvested from monolayer culture with 0.25% trypsin/EDTA (Sigma, St. Louis, MO). Trypsin was neutralized with 10% FBS in DMEM. Fibroblasts were harvested for experimentation until the 9^{th} passage (approximately 25 doublings). The ATCC product specification for this cell line states a proliferation capacity for 52 population doublings before the onset of senescence.

Preparation of Defined Medium

The following defined medium (free of serum and other mitogenic factors) was prepared: RPMI Medium 1640 (Gibco, Frederick, MD) supplemented with L-glutamine, 1x solution of Serum Replacement 1 (Sigma, St. Louis, MO) and 5ng/ml Sodium Selenite, 0.12mg/ml Pyruvate, 0.01mg/ml Insulin from bovine pancreas, and 5.5µg/ml Transferrin (SPIT medium supplement) (Sigma, St. Louis, MO). When indicated,

commercial preparations of human recombinant EGF were obtained from Sigma (St. Louis, MO).

Fluorescent assay to focus the projection image onto the bottom window of the flow cell

A photoreactive group (MeNPOC-thymidine) was covalently attached to a hydroxyl bearing glass slide in a reaction chamber using equal parts of a 50mM MeNPOC-thymidine and activator (Tetrazole) (Transgenomics, Omaha, NE) solutions. After rinsing the slide with 10ml acetonitrile)four times (for a total of 40ml) and drying the slide with Argon gas, I_2 oxidizer (Beckman Coulter, Fullerton, CA) solution was injected into the reaction chamber and allowed to react with any remaining –OH groups that did not bond with the photoreactive group (these groups left exposed would decrease the signal to noise by creating unwanted bonds with the phosphoramidite in later steps). The slide was again rinsed with 40ml acetonitrile and dried with argon gas. Then it was removed from the reaction chamber and placed in the flow cell chamber and mounted on the instrument. One Image was projected from the DMD with 365nm light for each adjustment to the flow cell stage in order to determine the focal plane (single mirror resolution can be located within a 10μm range). The slide was then taken out of the flow cell and put back into the reaction chamber to be probed with a 50mM solution of Cy3 phosphoramidite. The image was then visualized with a fluorescent scanner.

Seeding cells into the flow cell chamber

The flow cell, silicone o-rings and glass slides were autoclaved under dry cycle conditions. The flow cell was then assembled in a sterile tissue culture laminar flow hood. The chamber was rinsed with 20ml of defined medium before introducing

fibroblasts ($3x10^4$ cells/ml) suspended in DMEM supplemented with 10% FBS into the chamber. The chamber was placed inside a petri dish and put into a humidified incubator. After a sufficient amount of time to allow cells to adhere to the glass surface (approx. 4-6 h), the chamber was rinsed with 5 ml defined medium in order to wash away the serum containing medium. The cells underwent a 12 h serum starvation. At this point, the septum ports were connected and the chamber was immediately mounted on the instrument for experimentation.

Assembling the medium bottles for the instrument

The bottle lids with tubing were submerged in a 30% bleach solution for 10min. The liquid was also sucked into the tubing so that all surfaces were exposed to the bleach solution. After 10minutes, the lids and tubing were rinsed with sterile milli-Q water. The lids were then attached to glass bottles which had previously been autoclaved. Sterile culture medium was then added to each bottle. Two 0.2µm syringe filters were attached to the end of two of the tubing lines (one for introducing 5%CO_2, the other for ventilation). The third tubing line, reserved for fluid flow was capped.

Preparing the instrument for each experiment

The inlet and outlet ends of the tubing (normally connected to the flow cell) joined using a male-male luer lock connector in place of the flow cell. 30% bleach was pumped through the fluid lines and allowed to sit for 10minutes. After 10minutes, the tubing lines of the medium bottles were connected to the fluid and gas lines. 10ml of medium was pumped through the fluid lines to rinse away the bleach solution. The male-male luer lock connector was then removed and replaced with two 22gauge syringe needles which pierced the septum ports of the flow cell mounted on the instrument stage.

Culturing cells with intermittent exposure to EGF using the instrument

Defined medium containing 50ng/ml of a commercially available preparation of human recombinant EGF (bottle 1) was delivered at 2 ml/min for 3 minutes to the flow cell. After a 10 minute wait period, the growth factor medium was flushed away with 6ml of defined medium (bottle 2) at a flow rate of 2 ml/min. Each time the medium was replaced in the chamber, 5 ml of the type of medium being delivered was first shunted around the flow cell at 10ml/min to prep the lines for the medium delivery to the chamber. The defined medium was left in the chamber for 30 minutes. The procedure was repeated continuously throughout the experiment. At various times throughout the experiment, the flow cell was removed so that the number of cells in ten randomly selected fields could be counted visualizing phase contrast light microscopy. Upon removing the flow cell, the inlet and outlet lines were joined together with a male-male luer lock connector. New 22gauge syringe needles were used each time the flow cell was replaced.

In a control experiment, defined medium with 50ng/ml EGF (bottle 1) was introduced to the flow cell at 2 ml/min over 2 minutes. It was immediately washed away with defined medium from bottle 2 (6ml delivered at 2 ml/min). The defined medium remained in the flow cell for 30 minutes before repeating the cycle. Each time the medium was replaced in the chamber, 5 ml of the type of medium being delivered was first shunted around the flow cell at 10ml/min to prep the lines for the medium delivery to the chamber. Once again, the flow cell was removed at various times in order to count the number of cells in 10 randomly selected zones. The flow cell was removed and replaced as described above.

CHAPTER FIVE

CONTROL OVER CELL PATTERNING WITH LIGHT-ACTIVATED EGF USING AUTOMATED INSTRUMENTATION

Once it had been established that intermittent exposure to EGF will promote fibroblast proliferation, there was a basis for creating patterns of cells using spatially resolved activation of caged EGF. The goal was to establish a method to control activation of caged EGF via photolysis in a specific location of a culture of fibroblasts to stimulate proliferation of only those cells within the illuminated area. Cells outside of the illuminated area would receive no active factor and would thus withdraw from the cell cycle, leaving only the cells within the illuminated region viable. There were several challenges to meeting this goal; each was associated with light activation.

High doses of UVA can cause damage to mammalian cells (Berneburg, Grether-Beck et al. 1999). Therefore it was critical to determine an irradiation regimen that was able to cleave the caged compound from the light-activated growth factor but not cause cell damage or disrupt the growth cycle. Spatial activation of a soluble molecule meant that there was constant competition between the rate of photolysis and diffusion. In other words, as caged EGF was activated via photolysis, it would immediately begin diffusing away from the area of activation. So the faster relevant amounts of active EGF could be produced, the less concern there was with diffusion disturbing the spatial resolution. Therefore, not only did the irradiation regimen need to cleave the caging compound from the light-activated EGF without damaging cells, it needed to produce high enough concentration of EGF to stimulate proliferation while not damaging the cells.

5.1 Devlopment of parameters to control cellular activity using spatially resolved photolysis

To harness the capability for the spatially resolved control of cell behavior, a protocol of caged growth factor delivery and activation was needed to produce effective concentrations of activated growth factor on a time scale competitive with diffusion, but would not injure the cells with high input of UV light.

The relevant parameters were: wavelength to cleave the protective group from the protein, concentration of light activated EGF, light irradiation power (photolysis rate and extent of UV dose cells can sustain without damage), light irradiation period, rest period between pulses of illumination, and replenishment of light activated EGF (media replacement). The experimental and theoretical considerations that guided the choices for these parameters are summarized as follows:

5.11 Wavelength to cleave the protective group from protein

Nitrobenzyl derivatives have been widely used as photolabile protective groups which can be effectively removed by photolysis. The use of α-methyl-2-nitropiperonyl (MeNPOC) as a photolabile group, previously reported in the light-directed synthesis of nucleic acids (McGall 1997), has several advantages over other caging compounds for the purpose of the work described here. Photolysis of this group is cleaner and produces fewer complicated side products than other nitrobenzyl derivatives. Photoremoval of this compound can be done under near-UV illumination, as the absorbance of the MeNPOC chromophore (λ_{max}= 345 nm, ε= 5 x 10^3 M^{-1} cm^{-1}) becomes negligible at wavelengths above 400 nm (McGall 1997). The Mercury-Xenon lamp the instrument was equipped with was a convenient source of light in the appropriate wavelength range having an

emission peak at 365 nm. While the caging compound could be removed by photolysis at lower wavelengths, these were avoided due to potential of photochemically induced damage to cellular DNA (Cadet 1990).

5.12 Concentration of light activated EGF

For developing a method to create cell patterning, the growth factor concentration used was based on the experimentally determined relationship between concentration and proliferative activity for caged and photolyzed factor (Figure 3). In the concentration range of 25-50 ng/ml, the caged EGF stimulated little proliferation, whereas the photolyzed factor had near maximal activity. Because spatially localized photolysis must compete with diffusion to create spatially localized active material and because photolysis occurs as an exponential decay of caged material and cannot be carried out to completion on a time scale competitive with diffusion at biologically tolerated light power levels, the opportunity to create active concentrations of EGF is best at the upper end of that concentration range. Thus most of the experiments used 50 ng/ml caged EGF.

5.13 Projection Pattern

In the cell patterning experiments, the projection pattern was chosen so that it was possible to visualize the differences between cells within the illuminated and non-illuminated areas of the flow cell in a single experiment. The width of the pattern was chosen so that it was narrow enough to observe through the image field of view for one objective of the microscope, but large enough so that any effects from the light would be apparent. Rectangular images the full length of the DMD (13 mm) but varying widths (340 μm – 800 μm) were selected as projection patterns onto the flow cell. Patterning of

cell response was seen at both ends of that range (narrowest pattern shown in Figure 23) with rough correspondence between the cellular pattern and the image size.

5.14 Light irradiation power

The power and time of irradiation are based on the expected rate of photolysis (assuming the linear relationship between photolysis rate and light power that has been observed by others (McGall 1997), a mathematical estimate of diffusion coupled with photolysis developed for this project (Appendix A), and the amount of irradiation the cells could tolerate. Adjustment of the irradiation power achieved at the flow cell chamber affects the activation rate and dosage of light-activated growth factor.

The power levels tested during the development of the light-activation parameters were 0.7 mW/cm^2 and 12.0-14.6 mW/ cm^2 at the flow cell chamber. (The range of 12.0-14.6 mW/ cm^2 represents the maximum power obtainable during the course of these experiments, decreasing from 14.6 mW/ cm^2 to 12.0 mW/ cm^2 over the lifetime of a lamp. 12.0 mW/ cm^2 was selected because that level was conveniently reproducible irrespective of lamp usage level and optical system alignment). The half-life for photolysis at 0.7 mW/ cm^2 was 26 min, whereas for the higher power it was around 90 s. Two distinctive light-activation scenarios were created by the difference in half-lives: gradual (26 min half-life without diffusion) and pulsed (90 s half-life without diffusion) light-activation of EGF. (Note: More active factor was generated per unit time when diffusion brings untreated material into the illuminated region).

At the lower irradiation power (i.e. 0.7 mW/ cm^2), the rate of photolysis was slower (i.e. half-life longer), so the concentration of active material was slowly increased over time to reach relevant levels for stimulating cell behavior. A potential advantage of

this type of delivery was the ability to maintain steady, relevant amounts of active factor in the illuminated area. The mathematical estimate of diffusion coupled with photolysis (Appendix A) with power at 0.7 mW/ cm^2 suggested that diffusion would be slow compared to photolysis for a 26 min photolysis half-life, indicating that relevant amounts of active factor could be maintained in the illuminated area. However, as described in the following section 5.15 and in appendix B, irradiation at 0.7 mW/ cm^2 for periods of time expected to maintain relevant levels of active factor resulted in a change from spread to spheroidal morphology across the entire substrate, with cells in the illuminated region noticeably smaller than in non-illuminated regions. We interpreted these changes as resulting from cell damage and death, possibly due to UV-induced damage and heating of the substrate. By increasing irradiation power (second scenario), the half-life for photolysis was reduced, so the same concentration of active growth factor can be created in a shorter amount of time. This established a desirable relationship with regards to the competition between rate of photolysis and diffusion. In addition, short pulses of UV may provide time for the substrate to cool and for cells to recover from harmful UV effects between irradiation pulses. Light induced damage of cells has been shown to depend not only on total energy dose, but also on the temporal pattern of exposure (Berneburg, Grether-Beck et al. 1999). Delivery of relevant amounts of active factor was in shorter pulsed dosages as power increases so growth factor was available to cells for shorter periods of time before being diluted by diffusion. However, it was previously established that intermittent (pulsed) delivery of EGF stimulated cell proliferation (Section 4.21).

Both scenarios were tested using recombinant EGF and irradiation times that were expected to generate effective concentrations of active EGF to assess the tolerance

of cells for the different light-power scenarios. Outcomes for these experiments are described below and summarized in Appendix B.

5.15 Irradiation and recovery period

As stated above, the photolysis half-life was 26 minutes at 0.7 mW/cm^2 irradiation power, though more active factor was created in 26 minutes than suggested by this half life when unphotolyzed factor was continuously replenished to some extent by diffusion. Irradiation periods from 5 - 20 hours were tested and in each case there was a morphological change from spread to spheroidal (particularly, that cells within the illuminated area were smaller spheroids than those in non-illuminated regions), which was interpreted as cell damage and death. Since UV exposure can lead to the production of harmful singlet oxygen and hydrogen peroxide, the effects of which must be mitigated by normal cellular mechanisms, it was examined whether frequent rest periods (without illumination) would enable the cells to recover from harmful effects of UV exposure, also allowing the substrate to cool between irradiation periods. The irradiation power was reduced to 16 minute periods and 1 hour recovery periods without illumination. For this exposure, no morphological difference was observed between illuminated and non-illuminated regions, though there was still a decrease in cell density over time. In order to further reduce the illumination period, but still maintain relevant amounts of active EGF, the rate of photolysis was shortened by increasing irradiation power (as previously described).

With irradiation power increased to 12 mW/cm^2, two types of irradiation/recovery periods were tested: short, evenly spaced 15 s pulses or one long 90 s pulse followed by a shorter 30 s pulse. In the first type of dosage, there was a gradual

increase in the concentration of active factor in the illuminated area and the irradiation period was short to reduce cell damage from UV effects. The second type of delivery was expected to produce a relevant amount of active factor in one single pulse and allow a brief period for cooling and exchange of active and caged EGF into the region of activation by diffusion, so that a shorter second pulse further boosts the concentration of active factor in the illuminated area. For these parameters, no apparent death due to irradiation (as compared with long irradiation pulses) or difference between illuminated and non-illuminated regions was observed. Experimental summaries are listed in Appendix B.

5.16 Replenishment of medium (medium replacement)

During the studies to establish the cell culture parameters of the flow system, proliferation rates decreased when medium replacement occurred at intervals longer than 4 hours. Decreasing the half life to 28 s allowed frequent (4 hour) exchange of the medium. Additionally, only a small fraction of EGF would be photolyzed before replacement at this frequency with the size of illumination area used. Even with the constant illumination in migration experiments, only fractional amounts of EGF would be photolyzed before replacement. Therefore, frequent medium replacement promoted the ability to maintain a gradient of active EGF.

5.2 Cell patterning using light-activated EGF

Using the above parameters, cell patterning was achieved, described as follows. Defined medium containing light-activated EGF (50ng/ml) was introduced to a culture of NIH/3T3 fibroblasts uniformly distributed across the entire surface of the uncoated glass window of the flow cell chamber. A 340 μm wide rectangular strip was illuminated for

90s, followed by a 6 minute wait, then a second pulse of illumination for 30 s. This pattern of illumination was repeated hourly. The medium was replaced automatically every 4 hours, followed by a one-hour wait for the system to equilibrate before resuming the hourly illumination regimen.

After three days of this protocol, a clear rectangular strip of cells was visible in the position of illumination, shown in Figure 23. The region of highest cell density was somewhat narrower than the illuminated region (~300 μm). Outside of the illuminated region, few spread cells remain and a low density of spheroidal cells decreased with increasing distance from the illuminated region.

Control experiments using a commercial preparation of EGF showed no illumination-dependent variations in cell distribution. The cells remained spread and proliferated uniformly across the surface. When growth factor was omitted entirely from the medium, few cells survived for three days, a low density of spread and spherical cells were distributed without illumination-dependent variation. These control experiments suggested that the illumination-dependent variation in cell density was due to localized activation of the growth factor.

To ensure this effect was not the result of light-activated EGF bound to the surface, a control experiment was performed. In this experiment, cells were omitted from the chamber, but all other protocols from the patterning experiment were maintained. Defined medium with 50ng/ml light-activated EGF was delivered to the chamber and a 340 μm wide rectangular strip was illuminated for 90s, followed by a 6 minute wait, then a second pulse of illumination for 30 s. This protocol was repeated hourly with medium exchange very 4 hours. After three days of this protocol, the flow cell was disassembled

in a laminar flow hood and the lower chamber slide was washed in defined medium. The slide was then placed in a polystyrene tissue culture Petri dish and cells were seeded into the dish in defined medium. After enough time to allow for the cells to adhere to the substrate and spread, digital microphotographs were obtained of the distribution of cells on the glass substrate. The numbers of cells in the illuminated area and in an area of equal size outside of the illuminated area were counted. There were 58 cells in the area where illumination occurred and 63 cells counted in random zones (of equal area) outside of the area where illumination took place. The ratio of the number of cells in the illuminated region divided by the number of cells in the non-illuminated region is 0.921, close to 1. This result signifies that there was no illumination-dependent effect caused by surface binding. Thus, repetitive, localized activation of a diffusible growth factor has localized effects on cell behavior.

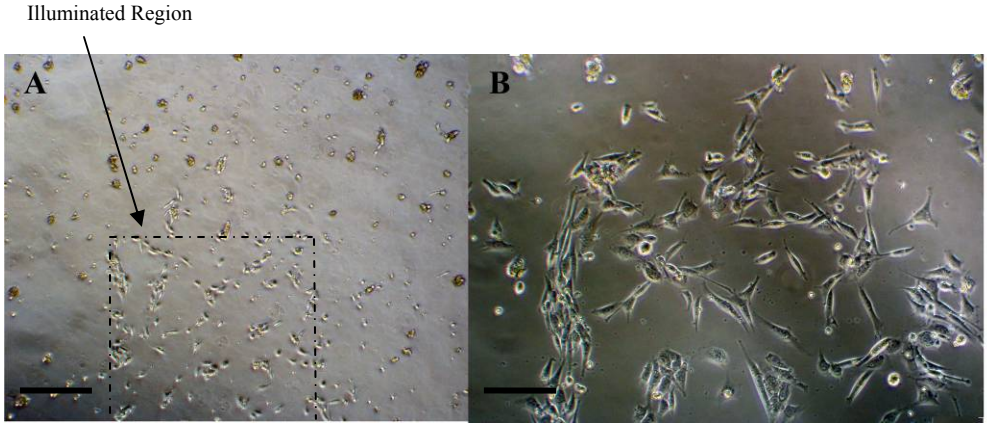

Figure 23: Spatially resolved activation of light-activated epidermal growth factor. **A.** Photomicrograph (no phase contrast) of the top portion of the illuminated region. Delivery of light-activated growth factor and illumination were as described in the text. The indicated vertical strip (dashed lines), 340 µm wide, was illuminated. Large dark features are aggregates of non-adherent, spheroidal cells, probably non-viable. Scale bar: 100 µm. **B.** Enlarged view of a portion of the lighted region with phase contrast for visualization of cell morphology. Scale bar: 50 µm.

5.3 Summary of results

Two distinct methods of photolysis were tested to determine parameters for spatially resolved activation of light-activated EGF. One method investigated using long illumination times at low power (0.7 mW/cm^2) levels. The other depended on creating relevant amounts of active factor in short bursts using at a higher power level (12-14 mW/cm^2). A systematic study investigating different UV irradiation exposure times for the two methods was performed using commercially obtained human recombinant EGF. The result of the study was that an irradiation regimen designed to provide relevant amounts of active EGF could be achieved with short irradiation bursts at higher power levels without damaging cells. Experiments determined to have no detrimental effect on fibroblast cell survival were repeated using 50ng/ml caged EGF to test the effects of spatially resolved activation.

Spatial patterning of fibroblast cells was achieved by projecting a rectangle illumination pattern for 90s followed by a 30s pulse 6 minutes later; repeated hourly for three days. A similar experiment using commercially obtained human recombinant EGF did not produce the same result. Additionally, a control experiment performed to measure the amount of surface binding of the light-activated EGF resulted in no illumination dependent variation in the distribution of fibroblasts. Thus, for the first time reported, cell patterning was achieved using a soluble light-activated growth factor.

5.4 Materials and Methods

General Cell Culture

NIH 3T3 fibroblasts (ATCC, CRL-1658) were maintained in Dulbecco's Modified Eagle Medium (DMEM; Gibco, Frederick, MD) with 10 % Fetal Bovine Serum (Sigma, St. Louis, MO). Fibroblasts were harvested from monolayer culture with 0.25% trypsin/EDTA (Gibco, Frederick, MD) and collected via centrifugation.

Defined medium with caged EGF

A stock solution of caged EGF was prepared as follows. The lyophilized protein was dissolved in equal volumes of Acetonitrile and milli-Q water with 0.05% TFA. Dilutions from this stock were made to obtain 200ml of defined medium containing 50ng/ml caged EGF.

Preparation of the flow cell

The flow cell, silicone o-rings and glass slides were autoclaved under dry cycle conditions. The flow cell was then assembled in a sterile tissue culture laminar flow hood. The chamber was rinsed with 20ml of defined medium before introducing 400µl fibroblasts ($3x10^4$ cells/ml) suspended in DMEM supplemented with 10% FBS into the chamber. Upon injection of the cell suspension, the port was flushed with 400µl medium so that cells did not remain in the port channel. The chamber was placed inside a petri dish and put into a humidified incubator. After a sufficient amount of time to allow cells to adhere to the glass surface (approx. 4-6 h), the chamber was rinsed with 5 ml defined medium in order to wash away the serum containing medium. The cells underwent a 12 h serum starvation. At this point, the septum ports were connected and the chamber was immediately mounted on the instrument for experimentation.

Preparing the medium bottles for the instrument

The bottle lids with tubing were submerged in a 30% bleach solution for 10min. The liquid was also sucked into the tubing so that all surfaces were exposed to the bleach solution. After 10minutes, the lids and tubing were rinsed with sterile milli-Q water. The lids were then attached to glass bottles which had previously been autoclaved. Sterile culture medium was then added to each bottle. Two 0.2μm syringe filters were attached to the end of two of the tubing lines (one for introducing 5%CO_2, the other for ventilation). The third tubing line, reserved for fluid flow was capped.

Preparing the instrument for each experiment

The inlet and outlet ends of the tubing on the instrument were connected using a male-male luer lock connector in place of the flow cell. 30% bleach was pumped through the fluid lines and allowed to sit for 10minutes. After 10minutes, the tubing lines of the medium bottles were connected to the fluid and gas lines. 10ml of medium was pumped through the fluid lines to rinse away the bleach solution. The male-male luer lock connector was then removed and replaced with two 22gauge syringe needles which pierced the septum ports of the flow cell mounted on the instrument stage. (Whenever the flow cell was removed from the instrument, during an experiment, the inlet and outlet lines were joined together with the male-male luer lock connector and new 22gauge syringe needles were used each time the flow cell was replaced.)

CHAPTER SIX

CONTROL OVER CELL MIGRATION WITH LIGHT-ACTIVATED EGF USING AUTOMATED INSTRUMENTATION

6.0 Developing a "Scratch Wound" Assay in the Flow Cell

To explore the application of our system to control cell migration, the scratch wound assay for cell mobility described in section 2.25 was adapted to the flow cell. The scratch wound assay relies on creating a cell-free region in an otherwise confluent culture for the cells to migrate into in order to heal the "wound." To perform quantitative, spatially dependent measurements in the flow cell, a method was developed to reproducibly create the border between the confluent cell population and the cell-free region in the same location. Reproducibility of the border was important since one of the variables involved in testing the ability to stimulate migration with spatially created gradients of light-active EGF was to determine the effect of the distance between the border of the cell population (leading edge) and the illuminated region on migratory response.

6.1 Confining fibroblasts to one half of the flow cell

The leading edge of the cell population was considered to be the cells on the border between the cell-populated region and the cell-unpopulated region of the flow cell. Establishing spatial localization of the illumination pattern from the leading edge presented a challenge. In initial experiments, cells were physically removed by scraping with a pipette tip, as in a standard scratch wound assay. However, the placement of the edge was not reproducible: there was a 2 mm range that the edge could be reproducibly located, the edge of the border was often uneven and many times there was a strip of cells

left behind in the scratched region. Furthermore, it was not possible to visualize the cells in the chamber while it was on the instrument in order to make adjustments to the location of the illumination pattern. Thus, a means of reproducibly isolating the cell population to an exact location within the chamber was required.

A method to accomplish this goal was developed during seeding using a mold made of a silicone elastomer (Dow Corning, Sylgard 184). The silicone elastomer mold is a fabrication of crosslinked polydimethylsiloxane (PDMS) described in the materials and methods section at the end of the chapter. The mold was made into a semi-circle shape, covering half the surface area of the flow cell. It adhered to the substrate during cell seeding, and was peeled off after the serum starvation step (just prior to starting each experiment). The mold restricted cells from adhering to one half of the surface area of the flow cell and created a well defined linear border. Importantly, the previous presence of the mold did not appear to interfere with cells migrating into the cell-free region, as long as the mold was not autoclaved (high temperature alters the properties of the mold). Others have also reported no noticeable change in migration resulting from using PDMS molds to create a mock "scratch wound."(Poujade, Grasland-Mongrain et al. 2007) Unless otherwise stated, cells were restricted to the half-circle on the inlet port side of the chamber. Using this method, the location of the leading edge could be maintained within ± 0.5 mm for each experiment. Since that tolerance was large compared to the μm-scale distances of interest, a second step was established. Before starting each experiment, microphotographs were taken of the flow cell chamber and stitched together using Adobe® Photoshop® Photomerge function. The compiled image was then superimposed on an image of the photolysis pattern in the flow cell produced with the surface chemistry

technique used for focusing the instrument projection pattern onto the chamber. From these images, the location of the photolysis pattern was adjusted so that the distance between the illuminated region and the leading edge of the cell population could be controlled in each experiment. This step decreased the tolerance that the location of the leading edge could be maintained to within ± 0.2 mm.

6.2 Determining the effect of fluid flow on cell migration

Even though the flow rate of 0.5ml/min did not appear to affect the vitality of the cell culture (Section 4.2), it was important to determine whether flow had any effect on cell movement across the substrate since cell migration was one of the behaviors the system was developed to study. In order to do this, a "scratch wound" assay was performed in the flow cell. Three fluid flow directions were tested in addition to no fluid flow. In the no fluid flow condition, the flow cell was placed within a Petri dish and kept in a humidified incubator during the course of the experiment.

The flow cell was assembled and defined medium was injected through one port to rinse the inner chamber. Dermal Fibroblast cells were then seeded into the flow cell at near confluence in DMEM supplemented with 10%FBS. After cells had adhered to the surface, the medium in the flow cell was replaced with serum-free defined medium then incubated overnight. The flow cell was then carefully disassembled so that cells could be removed (by scraping in these experiments) from one half of the flow cell to create a cell-free region. The cell-free region was positioned to be downstream of the remaining cell population, upstream of the remaining cell population or in line with the direction of fluid flow (Figure 24). The culture was washed twice with serum-free defined medium before reassembling the flow cell. Digital microphotographs were taken of the chamber and

stitched together using Adobe® Photoshop® Photomerge function. At this point the chamber was mounted on the instrument. Experiments were done with either 1ng/ml EGF or defined medium without growth factor. The medium in the chamber was replaced every 4 h. After 48h, the experiment was stopped and the flow cell was photographed again. The 48h composite photo was overlaid onto the 0h composite photo in order to identify the number of cells that migrated from the t=0h leading edge into the cell-free region. The number of cells that moved into the cell-free region was counted in 1mm incremental zones divided down the length of the leading edge. A result caused by fluid flow was expected to be identified from replicate experiments where a correlation between the numbers of cells that migrated in corresponding zones was observed.

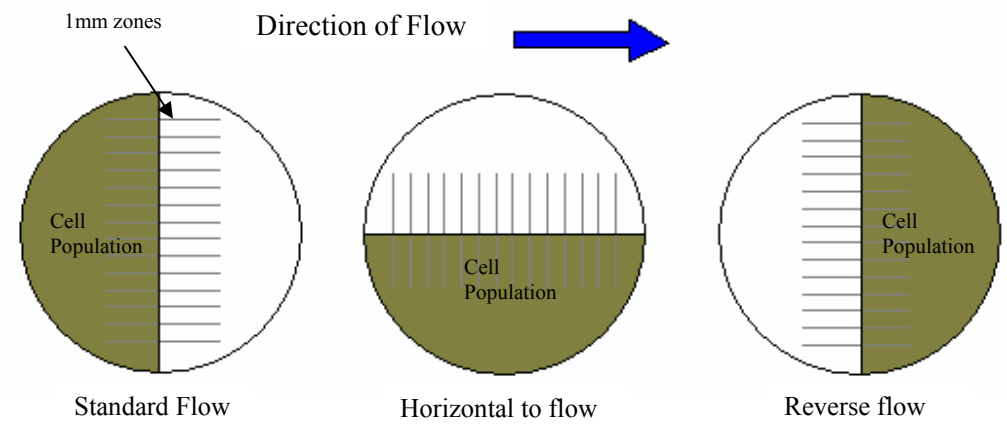

Figure 24: Test for flow effects on cell migration. Cell population distribution is for the t=0 time point.

For each type of flow (with and without growth factor), there was a large variance between zones in the number of cells migrating. The cells invaded the cell-free region in a non-uniform manner so that some zones had much higher cell counts than the neighboring zones. Even though this tendency was consistent between replicates, there

did not appear to be a trend for any particular zone that might indicate an effect due to the flow of medium. There were contiguous regions of high or low migration. The observation of this behavior, using the light microscope, was that the cells tended to move out in groups toward the cell-free regions. This observation is consistent with what others (Poujade, Grasland-Mongrain et al. 2007) have observed: the cells at the forefront of the finger-like columns of motile cells are "leader cells," which move into the cell-free zone, dragging a column of cells behind them. This effect can be seen in Figure 25, frequency diagrams of the number of cells per zone for the different fluid flow directions.

Bartlett's test for homogeneity of variance (Zar 1999) was used to test whether the variance was the same between different directions of medium flow. The null hypothesis for this test was that the variance was the same. When the test was applied to compare all of the different types of flow directions, the null hypotheses was accepted ($0.99<P<0.995$). Thus, no particular direction of fluid flow could be identified as having an effect on fibroblast migration from the results of this test, since there was an equal amount of variance. However, it is noteworthy that each direction of flow had similar variance to the "no flow" condition.

The test for homogeneity provided information about the overall variance in migration for each replicate, but did not provide insight regarding the zone-specific migration response. Thus, comparisons of the migration response between replicates for each zone were made using an ANOVA test for intraclass correlation. The test was performed on replicate experiments for the same direction of medium flow.

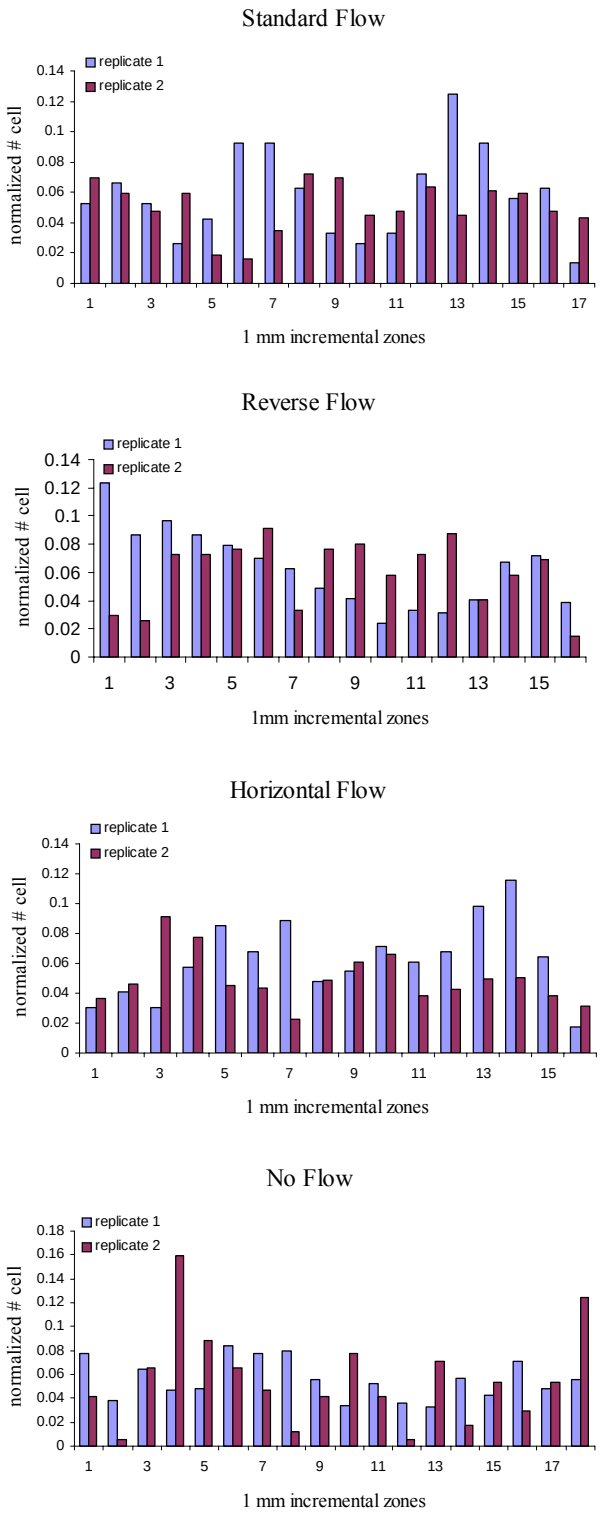

Figure 25: Fibroblast migration in the flow cell under different conditions of fluid flow.

For this analysis, the number of cells that migrated in each zone was normalized for the total number of cells that migrated. This was done to minimize migration differences from culture to culture variation of different passages of cell populations, since even though the variance within individual experiments may be the same; the total number of cells migrating for each experiment was typically not. The number of zones analyzed varied between fluid flow directions. This difference was due to inconsistencies in the scratch assay; for some instances cells were not removed along the edge of the chamber. When this occurred, those zones were omitted. Therefore, the number of zones analyzed for each direction of fluid flow is as follows: standard (17 zones), reverse (16 zones), horizontal (16 zones) and no flow (18 zones). The outcome of the ANOVA for each direction of fluid flow (including no fluid flow) was that there was no correlation among replicates (n=2) between the number of cells migrating in each zone. Table 1 lists the P value of the ANOVA test along with the correlation coefficient (r_1) for each type of fluid flow. The correlation coefficient describes the variability within zones compared to

Table 1: ANOVA intra class correlation

Fluid Flow Direction	r_1	P value
Standard Flow (n=17)	-0.222	0.828
Reverse Flow (n=16)	-0.137	0.701
Horizontal Flow (n=16)	-0.164	0.736
No Fluid Flow (n=18)	-0.071	0.613

between zones. A value of $r_1=1$, represents perfect correlation, whereas $r_1=0$ signifies no correlation. When r_1 reaches a negative value (-1 being the lowest value), the variability

within each zone (between replicates) is larger than the variability between zones (for a single experiment). This result further supports that there is not an effect of flow on corresponding zones for any of the fluid flow directions.

6.3 Method to test for surface binding of light-activated EGF to the substrate

An important feature of this technology is the ability to signal cell behavior using a soluble signal. Non-specific binding of the protein to the surface could lead to a situation where cells migrate along a gradient of bound EGF. Therefore experiments were completed to test for the degree of surface binding of the light-active EGF to the glass substrate. The flow cell was assembled with the silicone elastomer mold in place, identical to migration experiment preparation (except without cells). After flushing defined medium through the chamber, it was placed in a humidified incubator for 4 hours. After 4 hours, the chamber was disassembled in order to remove the elastomer mold. When the chamber was rinsed twice with defined medium, it was reassembled with septum ports in place. The chamber was then put on the instrument for experimentation. The experiment was repeated for medium containing either defined medium containing human recombinant EGF (1ng/ml), light-activated EGF (1ng/ml) or no growth factor. An illumination regimen of 3.5h constant illumination, followed by medium replacement and a 30 min rest period was repeated for 48 h. At this point, the chamber was removed from the instrument and disassembled in a sterile environment. The lower slide was washed with defined medium and then placed in a Petri culture dish with 15ml defined medium. Dermal fibroblasts were seeded into the dish at a density of 5000 cells/ml. The culture was incubated overnight before analyzing for preferential binding of cells to the previously illuminated area. Digital microphotographs were taken of the glass slide and

stitched together using Adobe® Photoshop® Photomerge function. The numbers of cells in the illuminated area and in an area of equal size outside of the illuminated area were counted.

Table 2 shows the number of cells bound to the surface in the illuminated and non-illuminated ("dark") area for the experiment. For each medium condition, the ratio of the number of cells adhered to the illuminated area vs. the number of cells adhered to the "dark" area was close to 1. This indicates that there was no photolysis dependent effect on protein binding to the substrate.

Table 2: Surface binding control	# cells in illuminated area	# cells in "dark" area	Ratio: illuminated/"dark"
Defined Medium	91	98	0.929
Human Recombinant EGF (1ng/ml)	103	107	0.963
Light-activated EGF (1ng/ml)	40	40	1

6.4 Test for effects of illumination alone on cell migration

A control experiment was done in the presence of human recombinant EGF to test for effects of illumination on cell migration. The flow cell was prepared as described in the materials and methods section at the end of the chapter. In this experiment, a cell-free region was created, oriented for the standard flow direction, using the PDMS mold. A rectangle shaped illumination pattern was positioned 1mm from the edge of the cell population. The image was projected continuously for 3.5h before replacing the medium with defined medium containing 1ng/ml human recombinant EGF. After a 30 minute rest period, the illumination regimen was repeated. This cycle was repeated for 48h before stopping the experiment. At 48h, digital microphotographs were taken of the flow cell and stitched together using Adobe® Photoshop® Photomerge. The compiled images for

0h and 48h were overlay so that the number of cells that migrated in 1mm incremental zones into the cell-free region could be counted. A t test was used to determine if the mean migration proximal to the illuminated region was significantly different from the mean migration distal from the illuminated region. For this test, 9 zones in each region (proximal or distal from the illumination) were compared, with 1 zone separating two the regions. The result was that the mean migration toward regions proximal and distal to the illumination was not significantly different (P=0.713). This result signifies that constant illumination does not have a location dependent effect on cell migration.

6.5 Stimulating cell migration using light-activated EGF

Gradients of light-activated EGF were established in an area proximal to where cells were allowed to remain in a "scratch wound" assay. The illumination pattern shape and size were varied to affect the photochemically created gradient. Adjustments were made to the distance between the illumination pattern and the cell culture, the time for photolysis, and the rest period between photolysis. Migration progress was assessed in 24h increments, by overlaying digital microphotograph images of the flow cell and counting the number of migrating cells in the illuminated and non-illuminated ("dark") regions. Comparisons were made between migration toward illuminated and "dark" regions for each illumination pattern and replicate. Similarity between replicates was also analyzed. Control experiments were done with either 1ng/ml human recombinant EGF (positive control) or defined medium (negative control).

6.51 Preparation of the flow cell

The flow cell was assembled with a semi-circular PDMS mold covering half of the lower window of the flow cell. The flow cell was rinsed with 20 ml defined medium

before introducing dermal fibroblasts (3 x 10^4 cells/ml) suspended in DMEM supplemented with 10 % FBS into the chamber. The chamber was placed inside a Petri dish and put into a humidified incubator. After a sufficient amount of time to allow cells to adhere to the glass surface (approx. 4-6 h), the chamber was rinsed with 5 ml defined medium in order to wash away the serum containing medium. The cells underwent a 12 h serum starvation. At this point, the top layer of the flow cell was removed so that the PDMS mold could be lifted from the chamber using sterile forceps. Then, the chamber was rinsed twice with defined medium before reassembled. At this point, the septum ports were connected and microphotographs were taken of the flow cell in order to locate the border of the cell population within the chamber. The images were stitched together using Adobe® Photoshop® Photomerge function. This was the 0h time point for each assay. The chamber was immediately placed onto the instrument for experimentation.

6.52 Brief illumination pulses with rest periods

Defined medium containing caged EGF (1 ng/ml) was introduced to a culture of dermal fibroblasts distributed across one half of the surface of the uncoated glass window of the flow cell chamber. Initially, the same protocol established for the cell patterning experiment was tested for stimulating cell migration. This consisted of a 4 hour repetition of 90 s illumination, 6 minute rest (without illumination), 30 s illumination followed by 52 minutes without illumination. At the end of the 4 hour cycle, the medium in the flow cell was exchanged. After 30 min without illumination, to provide time for turbulence to settle, the cycle was repeated. The irradiation power was maintained at 12mW/cm^2 and a circle shaped projection pattern with a 510μm radius was selected to create the

chemotactic gradient. Distances from the projection pattern to the leading edge of the cell population in a 0-2 mm range were tested.

This illumination protocol was expected to produce intermittent gradients of active growth factor. As previously noted, intermittent exposure to active growth factor stimulates fibroblast proliferation. However, under these conditions, no preferential migration toward the expected gradient was observed. In addition, no trends in alignment or differences in elongation between illuminated and non-illuminated zones were seen.

6.53 Stimulating Migration with Continuous Illumination and Effect of Distance between Illumination and Cells

As previously discussed, intermittent pulses of light were used to stimulate cell proliferation in an illuminated region, because continuous UV light exposure at relevant power and wavelength killed the illuminated cells. Fortunately, this UV damage was not a concern for these experiments, since the illumination was not directly on the cell population. Therefore, it was more desirable to increase the illumination time than to increase the concentration of growth factor, since at higher concentrations of growth factor there was less distinction between migration toward photolyzed and unphotolyzed light-activaed EGF (section 2.22). Larger projection patterns were also chosen in subsequent experiments to affect a larger proportion of cells in the chamber so that spatially

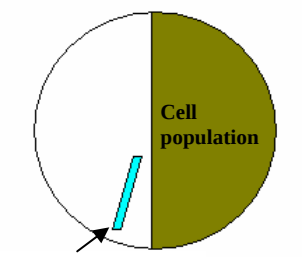

Figure 26: Diagonal Projection Pattern with respect to the t=0h border of the cell population.

dependent migration effects would be easier to recognize.

As a test of continuous illumination, a diagonal projection pattern was chosen (Figure 26). The geometry of the pattern was in the shape of a rectangle, 850μm x 6.3mm, positioned diagonally at a 164° angle relative to the leading edge of the cell population, projected from 0.5 mm at its closest end and 2 mm at its furthest end from the edge of the cell population. This pattern allowed for a range of distances between the cell population and the position of photolytic activation to be tested in parallel, within a single experiment. The illumination period was increased to 3.5h photolysis followed by medium replacement and a 30min rest period without illumination to allow any turbulence to settle before resuming illumination to repeat the cycle. The illumination cycle was repeated for 48 h, removing the flow cell in 24 h periods to photograph the migration progress. Migration was assessed by counting the number cells that migrated into the cell-free region per 1mm incremental zones along the leading edge. The experiment was repeated three times.

Frequency diagrams were constructed of the number of cells that migrated in each 1mm incremental zone, Figure 27. A non-random variation in the number of cells migrating was evident. Using the zones most distant from the region of illumination (>3 mm away) as an internal negative control, the mean and standard deviation of the "background" migration was determined. Cell migration in each individual zone was compared to this mean to assess if it is significantly larger than background with 95% confidence. The bars on the plots in Figure 27 for zones that are significantly different than background are colored.

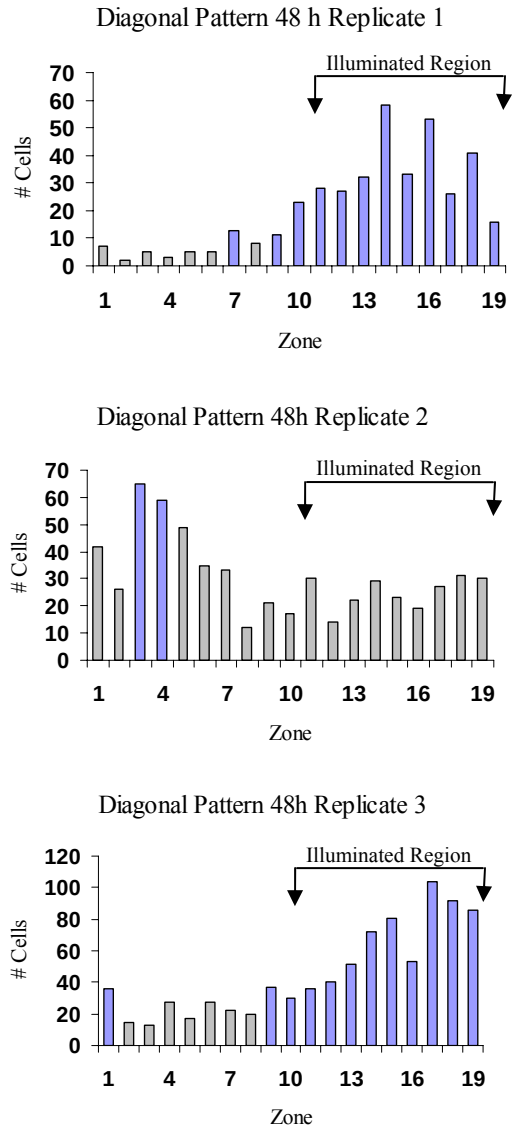

Figure 27: Frequency diagrams for replicate experiments with a diagonal illumination pattern used to photolyze light-active EGF. The chart shows the number of cells that migrated, after 48h, in each 1mm zone of the "dark" region (zones 1-9) or illuminated region (zones 11-19).

For replicates 1 and 3 the number of cells in each of the zones proximal to the illumination was higher than background. Similarly, the mean number of migrating cells

per 1 mm zone in the regions most proximal to the region of illumination (0.25-2.0 mm from illuminated area) was significantly higher than the mean number of cells per zone migrating in the regions furthest from the illuminated region (> 2.0 mm from illuminated area). The numbers of cells migrating in the region proximal to illumination and in the region furthest from illumination and the mean number of cells per 1 mm zone in each of these regions are summarized in Table 3. A t-test was used to compare these regions, the null hypothesis being that the migration was equal in both. P-values for this t-test are also listed in Table 3. For replicates 1 and 3, the null hypothesis is rejected (P<.0005), indicating that migration in the "illuminated' region is significantly different than migration in the "dark" region. Thus, the results in these replicates are consistent with cells responding to proximal illumination, putatively due to production of active EGF.

Table 3: Fibroblast migration response toward illuminated and dark regions for the diagonal illumination pattern.

Diagonal Pattern	Total and (mean) migration toward illumination region	Total and (mean) migration toward dark region	P value
Replicate 1	314 (34.9 ± 13.5)	59 (6.56 ± 3.6)	0.00017
Replicate 2	225 (25 ± 5.9)	342 (38 ± 17.5)	0.061
Replicate 3	615 (68.3 ± 24.2)	214 (23.8 ± 8.7)	0.0004

Different results were obtained in replicate 2 (figure 27) for both methods of comparing illuminated to dark zones. The number of cells migrating in the "dark" region was actually higher than that migrating in the illumination-proximal region. This difference, reversed from the other two replicates, was not statistically significant (P=0.061). This experiment points to effects that are beyond those controlled in our system. Nonetheless, the strong effects observed in the other two replicates (P values for

replicates 1 and 3 <<P value for replicate 2) are of higher statistical significance, especially when considered together, suggesting that light-induced migration is a genuine effect.

Another indication of the reproducibility of the observed cell response is obtained from an ANOVA test of intraclass correlation. This test provides a measure of correlation between corresponding zones in different replicates. Correlation in this test indicates the extent to which that the distribution of migrated cells is reproducible between experiments, i.e., not due to random effects. A correlation coefficient of 0.63 is found for replicates 1 and 3, whereas no correlation was found with replicate 2.

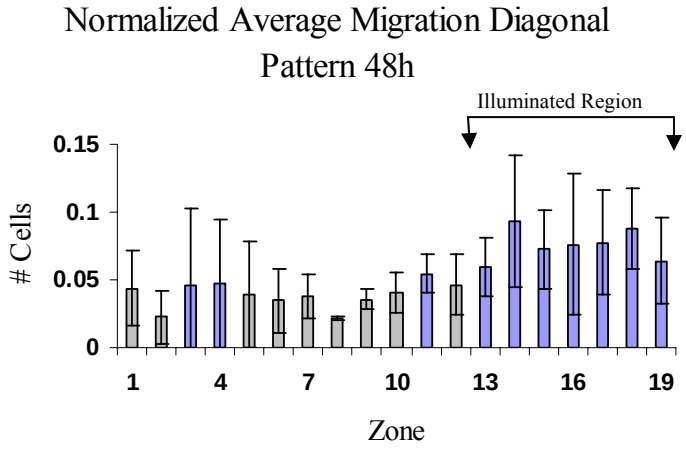

Figure 28: Normalized average migration for the diagonal projection pattern after 48h. The error bars represent the standard deviation.

The number of cells that migrated in each zone was normalized against the total number of cells that migrated in that replicate. This was done to remove variation between the total numbers of cells that migrated between replicates. The average of the normalized data was calculated for each zone and plotted in a frequency chart, shown in

Figure 28. The blue colored bars represent the zones where the average number of cells that migrated was significantly above the mean background with 95% confidence. Despite large standard deviation, the number of cells that migrated in zones proximal to the illuminated area is significantly different (higher) than the number of cells that migrated in zones distal to the illuminated area. There was 1.88 times more migration in zones proximal to the illuminated region than in distal zones.

Because the diagonal rectangle pattern allowed for a range of distances between the cell population and the position of photolytic activation to be tested in parallel, the results of this experiment were used to estimate a distance of separation (cells to illumination) that gives the highest response in cell migration. The number of cells migrating from the initial edge of the cell population into 1 mm zones is graphed versus distance of each zone from illuminated region for replicate 1 in Figure 29. In raw numbers of cells, the maximum migration occurred in the zone that was 1 mm from the illuminated region.

Microscopic inspection of the culture clearly revealed that the cells that reached the illuminated region died, as expected from previous experiments with continuous illumination. Thus, the full range of distance into which the cells could migrate increased with increasing distance between the initial edge and illuminated region, and the area of the zones that could be occupied by viable cells increased correspondingly. To account for this disparity, the cell density (i.e., cells/mm^2) was also considered as a function of distance (Figure 29). The cell density gradually decreased for distances greater than 1 mm, supporting the conclusion that this distance provides the best response in migration. It reinforces the conclusion that migration is dependent upon distance from the

illuminated region. This trend of cell density decreasing with increasing illumination distances above 1 mm is consistent for all replicates (including replicate 2, when only illumination-proximal zones are considered). Thus 1mm was selected as the distance between the projection pattern and the leading edge of the cell population (t=0h) for studying the fibroblast migration response of light-activated EGF gradients produced by different projection pattern geometries.

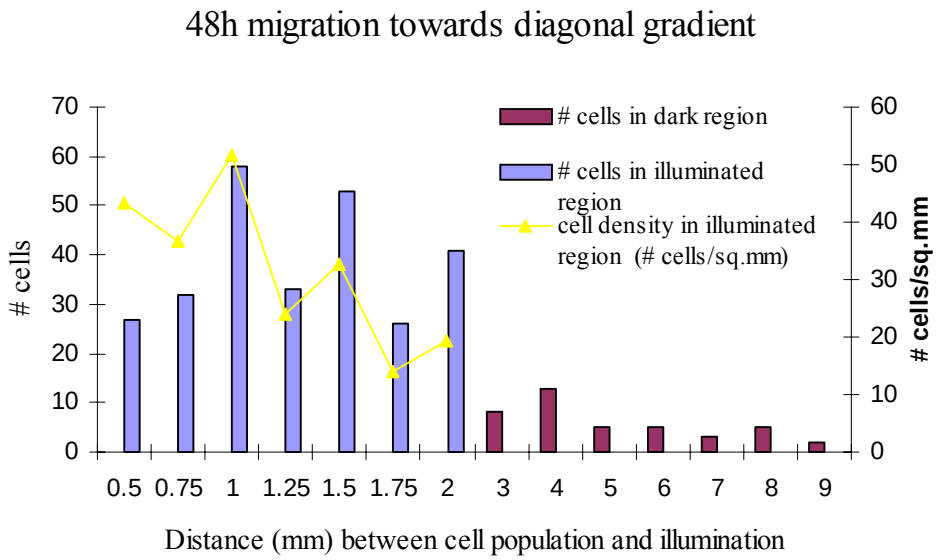

Figure 29: Density and number of cells migrated after 48h per zone for a given distance between the t=0h cell population border and edge of the illumination pattern "Dark" region data was included to provide perspective for the numbers of cells that migrate toward illuminated as opposed to "dark" regions of the flow cell.

6.6 Stimulating migration with different projection patterns

In addition to the diagonally placed rectangle in the previous section, two other shapes were projected: a vertical rectangle (850µm x 6.3mm, long axis 0° with respect to initial edge of cells) and a circle (1.5mm radius) (Figure 30). As with the diagonal rectangle, these regions were placed on one side of the center line of the chamber, thus providing an internal control, since the pattern only extended across a fraction of the width of the flow cell. Based on the results with the diagonal rectangle described above, the distance between the closest edge of the projection pattern and the leading edge of the cell population was 1 mm. These different patterns of light were expected to create different gradients of active EGF. Figure 31 shows the expected gradients for the different illumination patterns.

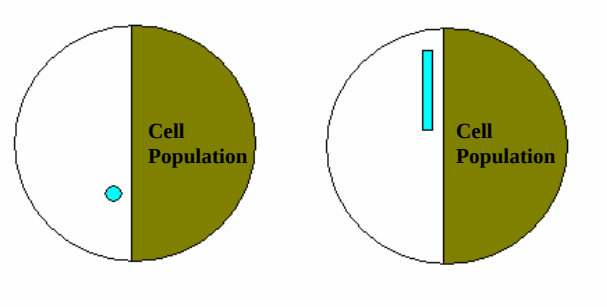

Figure 30: Circle and rectangle projection patterns with respect to the border of the cell population at t=0h.

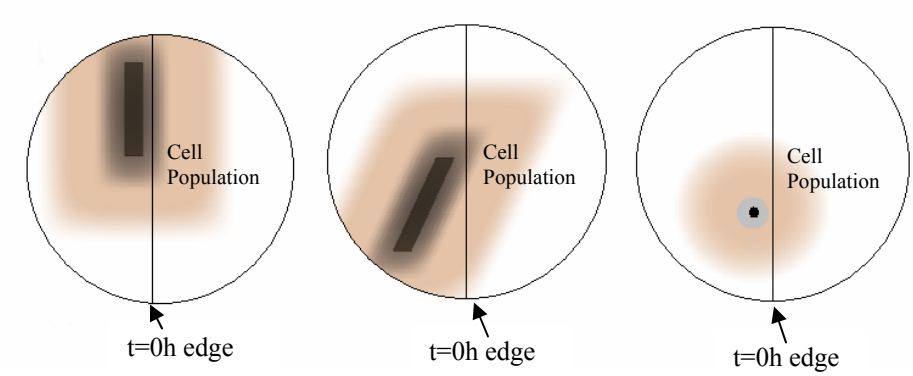

Figure 31: Expected gradient for each illumination pattern.

The rectangular pattern was expected to create a gradient that was uniform along the length of the rectangle at the initial edge of the cell population. The circular pattern was expected to create a gradient with a radial distribution.

Frequency diagrams for four replicates with the vertical rectangle are shown in Figure 32. As with the diagonal rectangle, a non-random variation in the number of cells migrating was evident, with the largest number of cells migrating within zones proximal to the illuminated area. Taking the 1 mm zones that are greater than 3 mm from illuminated areas as a negative control, the zones that are significantly different (confidence interval 95%) and proximal to the illuminated region are color highlighted.

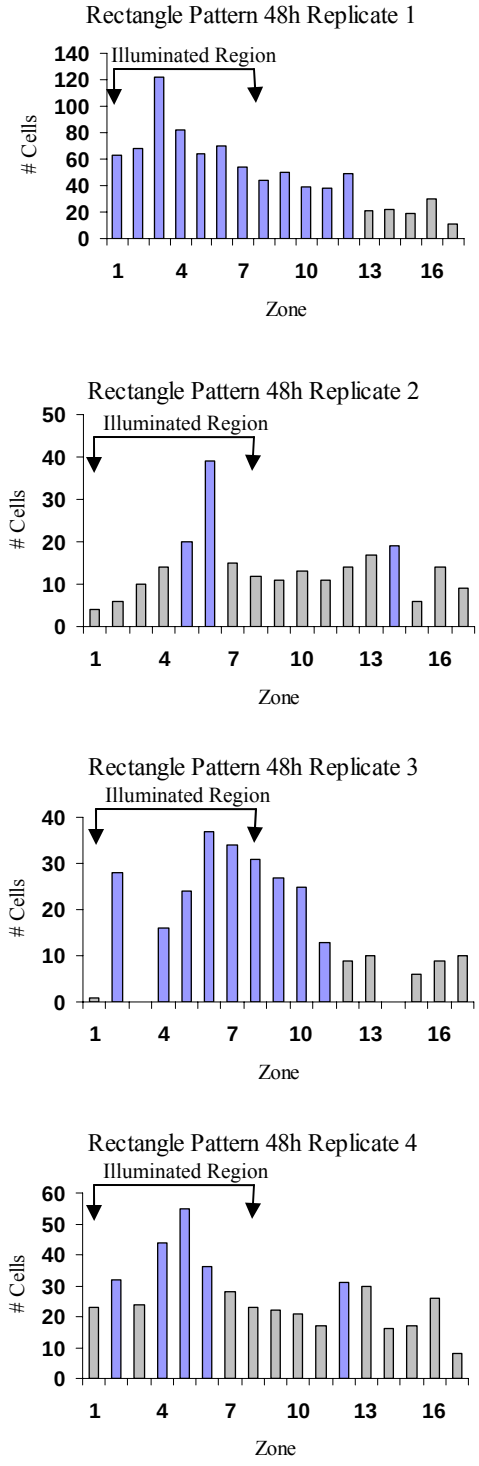

Figure 32: Frequency diagrams for replicate experiments with a rectangle illumination pattern used to photolyze light-active EGF. The chart shows the number of cells that migrated, after 48h, in each 1mm zone of the illuminated region (zones 1-8) or "dark" region (zones 10-17).

The numbers of cells migrating in the region proximal to illumination and in the region furthest from illumination and the mean number of cells per 1 mm zone in each of these regions are summarized in Table 4. A t-test was used to compare these regions, the null hypothesis being that the migration was equal in both. The P-values associated with this test are also shown in Table 4. For replicates 1 & 4, the null hypothesis is rejected ($P<0.05$), indicating that the migration in the "illuminated" region is significantly different than migration in the "dark" region. For replicate 2, the null hypothesis is accepted ($P=0.62$), as the number of cells that migrated in the illuminated region is only slightly higher than the number of cells that migrated in the "dark" region. The result for replicate 4 is less clear, acceptance of the null hypothesis is marginal ($P=0.078$). For this replicate there were twice as many cells that migrated in the illuminated region than in the "dark" region. Similar to what was observed using the diagonal projection pattern, the results are consistent with cells responding to the proximal illumination, though they also point to effects that are beyond those controlled in our system. However, once again, the strong effects of replicates 1 and 4 are of higher statistical significance, suggesting that the light-induced migration is a genuine effect.

Table 4: Fibroblast migration response toward illuminated and dark regions for the rectangle illumination pattern.

Rectangle Pattern	Total and (mean) migration toward illumination region	Total and (mean) migration toward dark region	P value
Replicate 1	567 (70.9 ± 23.5)	229 (28.6 ± 12.6)	0.001
Replicate 2	120 (15 ± 10.9)	103 (12.9 ± 4.2)	0.62
Replicate 3	171 (21.4 ± 14.4)	82 (10.3 ± 7.1)	0.078
Replicate 4	265 (33.1 ± 11.5)	166 (20.8 ± 7.9)	0.026

All four replicates were compared using the ANOVA test of intraclass correlation. The results indicated there was correlation in the distribution of migrated cells between experiments, $P<0.005$. The correlation coefficient was 0.47. This further supports that cells are responding to proximal illumination, ostensibly due to production of active EGF.

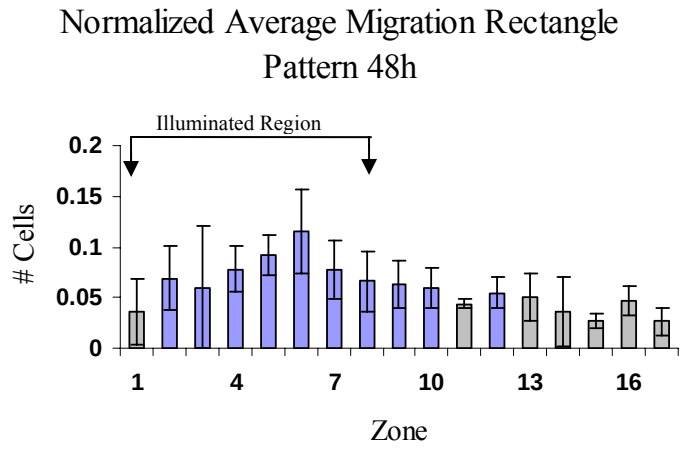

Figure 33: Normalized average migration for the rectangle projection pattern after 48h. The error bars represent the standard deviation.

Figure 33 is a frequency diagram of the average number of cells migrating in each zone for all four replicates. As previously done for the diagonal pattern, the number of cells that migrated in each zone was normalized against the total number of cells that migrated in that replicate. This was done to remove variation between the total numbers of cells that migrated between replicates. The blue colored bars represent the zones where the average number of cells that migrated was significantly above the mean background with 95% confidence. The number of cells that migrated in zones proximal to the illuminated area is significantly different (higher) than the number of cells that migrated

in zones distal to the illuminated area. There was 2.7 times more migration in zones proximal to the illuminated region than in distal zones.

Frequency diagrams for three replicates with the circle illumination pattern are shown in Figure 34. As with the other projection patterns, a non-random variation in the number of cells migrating was evident in at least two of the replicates, with the largest number of cells migrating within zones proximal to the illuminated area. Taking the 1 mm zones that are greater than 3 mm from illuminated areas as a negative control, the zones that are significantly different (confidence interval 95%) and proximal to the illuminated region are color highlighted.

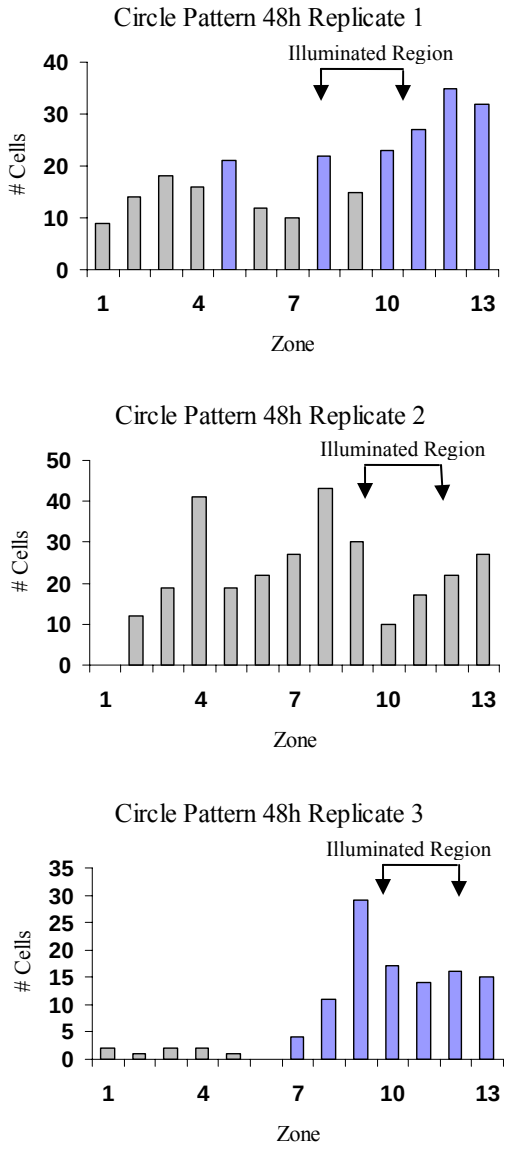

Figure 34: Frequency diagrams for replicate experiments with a circle illumination pattern used for photolysis of light-active EGF. The chart shows the number of cells that migrated, after 48h, in each 1mm zone of the "dark" region (zones 1-6) or illuminated region (zones 8-13).

Table 5 lists the numbers of cells migrating in the region proximal to illumination and in the region furthest from illumination and the mean number of cells per 1 mm zone

in each of these regions. A t-test was used to compare these regions, the null hypothesis being that the migration was equal in both. The P-values associated with this test are also shown in Table 5.

Table 5: Fibroblast migration response toward illuminated and dark regions for the circle illumination pattern.

Circle Pattern	Total migration toward illumination region	Total Migration toward Dark region	P values
Replicate 1	154 (25.7 ± 7.3)	90 (15 ± 4.3)	0.0144
Replicate 2	149 (24.8 ± 11.4)	113 (18.8 ± 13.4)	0.424
Replicate 3	106 (17.7 ± 5.6)	8 (1.3 ± 0.82)	0.00077

For replicates 1 & 3, the null hypothesis is rejected ($P<0.05$), indicating that the migration in the "illuminated" region is significantly different than migration in the "dark" region. For replicate 2, the null hypothesis is accepted ($P=0.42$), as the number of cells that migrated in the illuminated region is only slightly higher than the number of cells that migrated in the "dark" region. As in the results for the other patterns, the results using the circle illumination pattern are consistent with cells responding to the proximal illumination. Though once again, they point to effects occurring beyond those controlled in our system. However, once again, the strong effects of replicates 1 and 3 are of higher statistical significance, suggesting that the light-induced migration is a genuine effect.

Once again, an ANOVA test for intraclass correlation was performed on the replicates. The results for this pattern of illumination indicated there was no correlation in the distribution of migrated cells between experiments, $P<0.066$. The correlation coefficient for this test was 0.32. Even when the results of replicates 1 and 3 were compared, there was no correlation found. In fact, the correlation coefficient was only

slightly higher, 0.36. This result indicates that even though the migration response between illuminated and dark regions is statistically significant, there is less congruence in the response between replicates for this pattern of illumination.

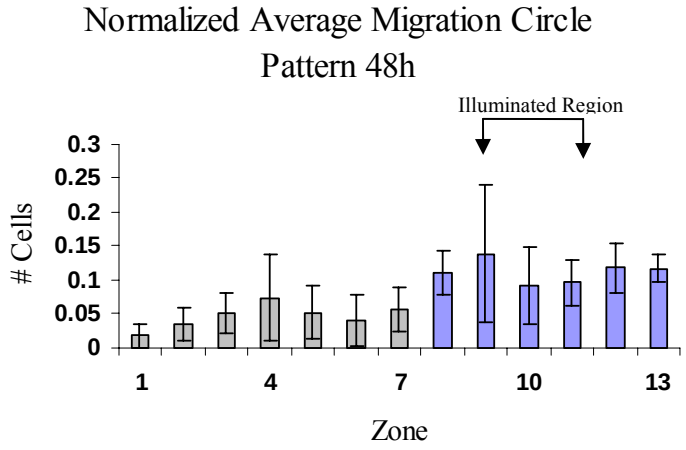

Figure 35: Normalized average migration for the circle projection pattern after 48h. The error bars represent the standard deviation.

As for the previous illumination patterns, the number of cells that migrated in each zone was normalized against the total number of cells that migrated in that replicate. The average of the normalized data was calculated for each zone and plotted in a frequency chart, shown in Figure 35. The blue colored bars represent the zones where the average number of cells that migrated was significantly above the mean background with 95% confidence. The number of cells that migrated in zones proximal to the illuminated area is significantly different (higher) than the number of cells that migrated in zones distal to the illuminated area. There was 1.92 times more migration in zones proximal to the illuminated region than in distal zones.

6.7 Stimulating Migration: Progressive Migration

After the initial 48 hours of illumination (for each pattern geometry), the projection pattern was moved further away from the original (t=0h) border of the cell population. Each projection shape was moved a different distance further from the original border of the cell population. The diagonal projection pattern was moved an additional 0.5mm, the circle pattern was moved another 1mm and the rectangle was moved 1.5mm further away from the original border of the cell population.

The number of cells that migrated was counted for the same 1mm increments measured at the 48h time-point. Corresponding regions, proximal and distal to the illumination, were compared at the different time points. Table 6 summarizes the additional number of cells that migrated into the illuminated and "dark" regions 24h after the projection pattern was moved further away (between 48h-72h) and the ratio of the total number of cells in the illuminated region to the total number of cells in the "dark" region. The results for the third replicate of the circle illumination pattern were excluded due to the occurrence of bacterial contamination at this latter time point (no contamination was present at the 48h time point).

Additional migration toward the illuminated region was not balanced by additional migration toward the "dark" region. A t test was used to compare the mean migration toward the illuminated and "dark" region for each experiment at the 72h time point. The resulting p-values are listed in Table 6. Only two experiments resulted in a significant difference between the mean migration for the illuminated and "dark" regions; replicate 2 of the circle and replicate 1 of the rectangle. In the case of replicate 2, for the circle illumination pattern, the total number of cells that migrated in the "dark" region

was higher than the total number of cells that migrated in the illuminated region. Recall, that this was also the only experiment for the 48h time point that resulted in more cells migrating toward the "dark" region than toward the illuminated region. For replicate 1 of the rectangle projection pattern, even though the mean migration toward the illuminated region was still significantly higher than the mean migration toward the "dark" region, the significance decreased over time from P=0.001 to P=0.011.

Table 6	Number of additional cells that migrated between 48h and 72h		Ratio of the total number of cells: (illuminated/dark) at 72h	t test P value
Shape	illuminated region	dark region		
Circle	17	143	0.734	0.21
	120	290	0.667	0.033
Rectangle	-86	339	0.818	0.22
	82	44	1.06	0.29
	80	24	2.37	0.060
	132	201	1.08	0.57
Diagonal	-131	26	1.84	0.011
	147	87	0.764	0.50
	-161	79	1.55	0.064

A frequency diagram for one of these experiments (the third replicate of the diagonal projection pattern) is shown in Figure 36. The diagram shows the migration per 1mm zone for both the 48h time-point (migration toward the first projection) and 70h time-point (migration toward the second projection). It is apparent from the figure that the difference between migration toward the illuminated and dark regions is diminishing. It is unknown whether the number of cells decreased in the illuminated area due to cell death or retreated back toward the cell population. There was no evidence to suggest that the cells in the illuminated region migrated toward the dark region at this later time point since the distance the cells would have to travel would be further than the distance they

traveled over the entire time span of the experiment. These results suggest that it was not possible to affect migration using light-active EGF with progressive patterns of photolysis over a 72h time span under these conditions.

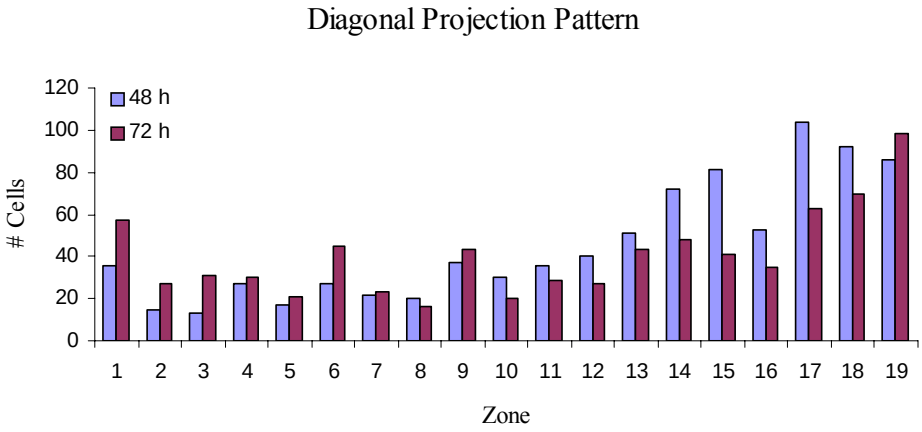

Figure 36: Progressive migration using the diagonal projection pattern, 3rd replicate. Zones 11-18 were nearest to the illumination pattern. Migration for each zone is shown for 48h (blue bars) toward the first projection pattern, after which, the pattern was moved an additional 0.5mm away from the cell population. The resulting migration after 72h in response to increasing the distance is also shown (magenta bars).

6.8 Materials and Methods

Defined medium with caged EGF

A stock solution of caged EGF was prepared as follows. The lyophilized protein was dissolved in equal volumes of Acetonitrile and milli-Q water with 0.05% TFA. Dilutions from this stock were made to obtain 200ml of defined medium containing 1ng/ml caged EGF.

General Cell Culture

Human Foreskin Fibroblast (HFF; CRL 2522) cells were maintained in Dulbecco's Modified Eagle Medium (DMEM; Gibco, Frederick, MD) with 10 % Fetal Bovine Serum (FBS; Sigma, St. Louis, MO). Prior to reaching confluence, the fibroblasts were harvested from monolayer culture with 0.25% trypsin/EDTA (Sigma, St. Louis, MO). Trypsin was neutralized with 10% FBS in DMEM. Fibroblasts were harvested for experimentation until the 9^{th} passage (approximately 25 doublings). The ATCC product specification for this cell line states a proliferation capacity for 52 population doublings before the onset of senescence.

Procedure for making PDMS mask

A two-part PDMS solution was mixed per the manufacturer's protocol in a 10:1 ratio. The mixture was poured into the silicone o-rings used in the chamber on the surface of a clean glass slide (3 per slide). The slide was placed onto a hot plate and warmed for 10 minutes until solidified. The mold was cut using a razor blade into a semi-circle, the o-ring was cut off using a scalpel.

Preparing the flow cell for a scratch wound assay

The flow cell, silicone o-rings and glass slides were autoclaved under dry cycle conditions. The PDMS mold and tweezers were sprayed with 70% ethanol and placed in a tissue culture laminar flow hood. The flow cell was then assembled in a sterile tissue culture laminar flow hood with the PDMS mold in place covering half of the lower slide.The chamber was rinsed with 20ml of defined medium before introducing 400µl fibroblasts ($3x10^4$ cells/ml) suspended in DMEM supplemented with 10% FBS into the chamber. Upon injection of the cell suspension, the port was flushed with 400µl medium so that cells did not remain in the port channel. The chamber was placed inside a petri dish and put into a humidified incubator. After a sufficient amount of time to allow cells to adhere to the glass surface (approx. 4-6 h), the chamber was rinsed with 5 ml defined medium in order to wash away the serum containing medium. The cells underwent a 12 h serum starvation. At this point, the septum ports were connected and the chamber was immediately mounted on the instrument for experimentation.

Assembling the medium bottles for the instrument

The bottle lids with tubing were submerged in a 30% bleach solution for 10min. The liquid was also sucked into the tubing so that all surfaces were exposed to the bleach solution. After 10minutes, the lids and tubing were rinsed with sterile milli-Q water. The lids were then attached to glass bottles which had previously been autoclaved. Sterile culture medium was then added to each bottle. Two 0.2µm syringe filters were attached to the end of two of the tubing lines (one for introducing 5%CO_2, the other for ventilation). The third tubing line, reserved for fluid flow was capped.

Preparing the instrument for each experiment

The inlet and outlet ends of the tubing (normally connected to the flow cell) joined using a male-male luer lock connector in place of the flow cell. 30% bleach was pumped through the fluid lines and allowed to sit for 10minutes. After 10minutes, the tubing lines of the medium bottles were connected to the fluid and gas lines. 10ml of medium was pumped through the fluid lines to rinse away the bleach solution. The male-male luer lock connector was then removed and replaced with two 22gauge syringe needles which pierced the septum ports of the flow cell mounted on the instrument stage.

CHAPTER SEVEN

DISCUSSION

Achieving control over cell behavior with spatial and temporal resolution is of major importance in the field of Tissue engineering. By using a soluble molecule, whose activation can be controlled in time and space, a method for achieving dynamic control over cell behavior can be created. Accomplishing this level of influence over cell behavior is critical for generating complex tissues and organs ex vivo. The work presented here describes a first step towards the development of such a technology. For the first time, a light-activated growth factor has been synthesized and used to influence cell behavior.

The experiments performed in the incubator environment established that light-activated EGF after photolysis stimulated proliferation and migration activities in fibroblasts, whereas before photolysis little to no activity was stimulated. In the proliferation studies, the doubling time for the cell population in the presence of light-activated EGF after photolysis was similar to the doubling time for the cell population in the presence of human recombinant EGF. In the migration assay, there was twice as much migration toward the light-activated EGF after photolysis than before. These results suggested that localized activation of light-activated EGF would result in stimulating a cellular response in the cells proximal to the area of activation but not in areas distal to it. The concentration profiles determined from these assays established the starting point to determine whether spatially resolved activation (via photolysis) of light-activated EGF would also result in spatially resolved control over proliferation and migration activities.

Automated instrumentation offers a high degree of control over timed delivery and activation of the growth factor, eliminating the need for an operator to be present during the entire process. Thus, to aid in the investigation of spatially resolved control over cell behavior using light-activated EGF, an automated instrument was designed, built and characterized. High resolution photolysis patterns on the size scale of a human cell were achieved. In addition, cell cultures could be maintained over days using this device.

Even though the instrument was constructed specifically to aid investigations using light-activated growth factors, the instrument is flexible enough to be used with other technologies. The instrument could be used for investigating the effects of other light-activated molecules on cells. Additionally, the high resolution offered by the optical component can be used for a variety of surface patterning techniques achieved with photochemistry. Furthermore, different filters can be adapted into the optical system to test how various wavelengths of light affect cells. The tissue culture component of the instrument also offers a variety of features which can be adapted for investigations of other cell lines. Multiple media types can be delivered to the heated chamber, as demonstrated in the proliferation experiment that investigated intermittent exposure of EGF on fibroblasts. Also, the medium can be delivered at variable speeds. The fluid dynamic environment has different affects on cell morphology and vitality. Certain cell lines, such as chondrocytes, respond favorably to fluid induced shear. Thus, the instrument is ideal for studying the fluid dynamic environment factors on cell culture. Since the instrument features the ability to control multiple components simultaneously, one or more of the culture conditions can be tested or adjusted in a single experiment.

Effective protocols for carrying out photolysis of light-activated EGF, during cell culture, without damaging cells were determined. Cell patterning was achieved using one of these protocols to activate 50ng/ml caged EGF via spatially resolved photolysis. Control experiments supported that the effect was due to photolysis of the soluble caged molecule and not an artifact of surface binding or of the illumination. This proves that light-activated versions of soluble growth factors can be created and used to influence cell behavior with defined spatial resolution. Ideally, this aspect of the technology can be developed to create three-dimensional patterns of cells within different matrices. For this to be possible, the matrix would need to be sufficiently transparent so enough light can be transmitted to photolyze the caged growth factor. The structure and composition of the matrix would also need to be uncompromised by UV light. These investigations would need to examine not only stimulating proliferation within the matrix but also the ability to induce migration and remodeling in response to the light-activated growth factor. Therefore, as a progression towards that goal, after achieving two-dimensional cell patterning, efforts were turned towards influencing two-dimensional cell migration using resolved photolysis of light-activated EGF.

Preferential migration toward localized gradients of light-activated EGF created by photolysis was achieved using three different illumination projection patterns over a 48h timeframe. In each case the projected illumination pattern was located at a distance of 1mm away from the edge of the cell population. A significant reproducible effect on cell migration, requiring the light-activated factor and illumination was observed for each of the tested illumination shapes. The number of cells migrating per zone was normalized for the entire number of cells migrating in the corresponding replicate. The normalized

average number of cells that migrated per zone was then calculated for each illumination shape. For each shape tested, the number of cells that migrated proximal to the illumination pattern was roughly two times higher than the number of cells that migrated in the region distal to the illumination pattern. This is consistent with the measured migration difference between caged and photolyzed EGF in the scratch wound assays performed in the incubator environment.

The overall normalized average of all of the replicates resulted in a significant difference between the numbers of cells that migrated proximal and distal to the area of photolysis for each projection pattern. However, in a few of the replicate experiments, there was not a significant difference in the number of cells that migrated in the two regions. The fact that there was some difficulty reproducing the effect signifies the complexity of influencing cell migration under these circumstances. These results suggest that there are unknown variables influencing migration that could not be entirely controlled for in these experiments. These variations might be due to differences between passages of cell populations. Another possibility could be that the light-activated EGF was improperly folded in those experiments. A likely possibility is that environmental factors, such as vibration, played a role in disrupting the result. Each of the experiments where little difference existed between the numbers of cells that migrated proximal and distal to the illuminated region took place during the same days of the week, whereas none of the experiments where there was a significant difference were performed during these days. Vibrations in the building or due to other instruments in the room may have influenced the results of these experiments since the turbulence would disrupt the resolution of the photolysis signal. This possibility should be factored into future

experiments by measuring the vibration on the instrument over the course of each experiment. There are several commercially available vibration meters for this purpose.

The previous migration studies in the incubator may also provide some insight. The "scratch wound" assay is more representative of the experiments performed using the instrument than the Boyden chamber assay. The results of migration experiments performed using the "scratch wound" assay were somewhat less robust than those done using the Boyden chamber. The difference in the migration response towards light-activated EGF before and after photolysis was just over two-fold in the "scratch wound" assays done in the incubator. However, in the Boyden chamber there was a much larger difference. Thus, creating an environment in the flow cell more like that of the Boyden chamber experiments might afford a greater difference between the migration response proximal and distal to the area of photolysis. The membranes in the Boyden chamber assay were coated with collagen. It is possible that the coated membrane bears closer resemblance to the native matrix environment or simply that the collagen coated membrane provides a better surface for the cells to adhere and move along compared to the clean glass surface in the flow cell. Therefore, future studies should investigate whether surface coating or the presence of a gel matrix would enhance the migration response to photolyzed EGF. Nevertheless, the achieved migration response to controlled localized gradients of photolyzed EGF provides motivation that further development of this technique could result in a more robust response.

After 48h, the illumination gradient was moved further from the population of fibroblasts. At 72h, the difference between migration toward the illuminated and dark regions began to diminish. In five out of eight cases, the migration toward the illuminated

area still increased, though only slightly. Decreased or slowed migration toward the illuminated region suggested that the chemotactic gradient created by the illumination pattern was moved to a distance beyond what the cell population could sense. This was in large contrast to the increase in migration that the dark region experienced. It was this increased migration toward the dark region that resulted in the migration difference between the illuminated and dark areas becoming diminished. Even if the illumination pattern had been moved beyond what the cell population was able to sense, it does not explain why cells would continue to migrate into the cell-free area of the dark region, but not the illuminated.

It has been reported (Poujade, Grasland-Mongrain et al. 2007) that migrating epithelial cells in the presence of low concentrations of hepatocyte growth factor (HGF) do not exhibit the highly directional migration that is typical of leader cells dragging follower cells behind them in finger-like projections. Leader cells are characterized by well defined focal adhesions at their leading edge and a loss of subcortical actin. Instead, the finger-like characteristic along the border of the scratch wound is less apparent when HGF is present, cell movement becomes scattered. It is not certain if, in the presence of HGF, all of the cells along the edge became leader cells. Poujade et al suggested that an entirely different mechanism of migration might be responsible for this difference in behavior. A similar phenomenon might be occurring during the progressive migration experiments with light-activated EGF. The fibroblasts in the dark region continued their direction of movement into the cell-free region, which is typical of highly directional leader cells pulling follower cells behind them. While cells nearest the illuminated region suddenly experienced a decrease in growth factor when the gradient was moved further

away and decreased their movement into the cell-free region, which suggests cells in the two areas were migrating due to different stimuli. This interesting result supports the usefulness for using this technology to study cellular systems. EGF also stimulates migration in epithelial cells. Therefore, future investigations of using light-activated EGF to stimulate epithelial cell migration may shed some light on the hypothesis that different mechanisms of migration are involved with and without the presence of growth factor. These studies should include fluorescent microscopy techniques to view the actin and focal adhesions of cells in the two areas.

For this technology to become a more valuable tool for tissue engineering or as a means of studying cellular systems greater influence over cell behavior for longer periods of time must be achieved. By increasing the difference between the cellular response to photolyzed and caged EGF, greater control over cell behavior can be accomplished. As previously mentioned, investigations using different surface coatings or matrix environments may improve the cellular response in terms of migration. Expanding this technology into the three dimensional, gel matrix environment is critical for this technology to be used as a tool for engineering tissues. The greatest benefit this platform offers is that since the light-activated growth factor is a soluble molecule, not attached to the substrate, native matrices can be used. Therefore, developing this area of the technology would secure its place among the most valuable tools for manipulating cell behavior. It would also provide a new technique for investigating matrix remodeling and contraction.

Another consideration for future studies on migration has to do with the length of time the experiment is carried out. While dense populations of cells will create their own

extracellular matrix and mitogenic factors, further supplementation may be necessary for the overall health of the culture. The migration experiments were carried out over the duration of three cell cycles at essentially too little concentration of EGF to maintain proliferation. Thus, in the future, intermittent pulses of either human recombinant EGF or light-activated EGF with brief photolysis pulses over the entire cell population may be beneficial.

It is also worthwhile to investigate how other cell types respond to light-activated EGF. While fibroblasts are responsive, there was a large variation between each passage of the cells regarding the degree of activity stimulated by light-activated EGF before and after photolysis. Another cell line may exhibit a greater response with less variation between passages. This would simplify making improvements to the technology, especially if there is less noise in the cellular response to light-activated EGF.

A future goal in the development of this technology is the synthesis of additional light-activated growth factors. More cellular behaviors could be controlled with a repertoire of light-activated growth factors to choose from. In addition, utilizing multiple light-activated growth factors simultaneously may provide the desired boost to create a larger difference between cellular response to photolyzed and caged growth factor since two or more growth factors are often involved in stimulating behavior. An alternative method to boost control over cell behavior is to investigate caging multiple residues during synthesis of the light-activated growth factor. However, adding more caging groups increases the complexity of the protein synthesis and may cause improper folding, due to the extra bulk, which could reduce activity. Therefore other alternatives to gain greater control over the cellular response will be investigated first.

In conclusion, the overall result of this work supports the rational for using light-activated growth factors for controlling cell behavior. Though the cellular response to photolyzed EGF was not always as strong compared to human recombinant EGF, the work described here shows that localized activation of caged EGF can affect cell behavior with spatially resolved dependence using this technology. These studies build a foundation for investigating and controlling cell behavior ex vivo. Future studies should expand upon these findings to improve this control and enable sophisticated tissue engineering.

APPENDIX A
Mathematical Estimation of Spatial Control with Diffusible Factors

The impact diffusion has on using soluble molecules to provide localized signaling diminishes resolution. During photochemical activation there will be a constant exchange of active and un-activated growth factor as the two diffuse into and away from the illuminated region. So diffusion and activation are united in the system and must be regarded as such to gain insight into the spatial and temporal distribution of active factor. A mathematical model describing simultaneous diffusion and photolysis was created to guide experimental design to determine the resolution that can be expected from a light-activated growth factor strategy.

In this model, photolysis was treated as a first-order process that converts chemical species A (i.e. caged growth factor) into two chemical species, B and C (i.e. activated growth factor and cleaved protecting group) upon photolysis. The change in concentration of A via photolysis is dependent on its photolysis rate constant, c, as a function of position, x, and time, t.

$$\frac{\partial[A](x,t)}{\partial t} = -c[A](x,t)$$

Diffusion can be represented mathematically as a partial differential equation which describes density fluctuations in a material. Since non-uniform distributions tend to distribute themselves in such a way as to produce uniformity, it is reasonable to assume that the flux density is proportional to the concentration gradient. Since diffusion will be distributed equally in all directions, the model can be simplified by analyzing diffusion in one dimension.

The concentrations of B and C can be regarded as the negative change in concentration of A. Diffusion of A and B can be described as:

$$\frac{\partial^2 u(x,t)}{\partial x^2} = \frac{1}{k}\frac{\partial u(x,t)}{\partial t}$$

where u is the time- and position-dependent concentration of a particular species and k is its diffusion coefficient. Since A, B and C are physically confined within the tissue flow chamber; diffusion must obey the boundary condition:

$$\left.\frac{\partial u(x,t)}{\partial x}\right|_{boundaries} = 0$$

The model solves a set of differential equations for changing concentrations based on diffusion and photolysis within those limits. This model was used to describe a variety of illumination schemes (pulsed and constant) in order to determine an optimal regimen based on the relationship of active growth factor to total growth factor as a function of time. The behavior was modeled along a single dimension of the flow cell (1.6 cm long, 100 element array), leading to a positional mesh size of 161.6 μm. Snap shots of the distributions of A and B can be output at any time throughout the simulation. An example of the model output is shown in Figure 37. In this simulation photolysis was analyzed at 2 mW/cm^2 of a region 162 μm for four half-lives (32 min), followed by diffusion without photolysis for 28 minutes. The cycle was repeated for 5 hours. The relative concentration of deprotected factor is plotted as a function of time for three different areas within the flow chamber: the illuminated region, the adjacent 162 μm region and the distant 162 μm region (808 μm from the edge of the illuminated region). This analysis predicts that significant concentrations of active growth factor can be

maintained with intermittent illumination along with diffusion. It also indicates that spatial resolution is maintained in relative growth factor concentrations. The information from these simulations is useful in selecting illumination and washing times as starting points in experiments to optimize photochemical control over cell behavior.

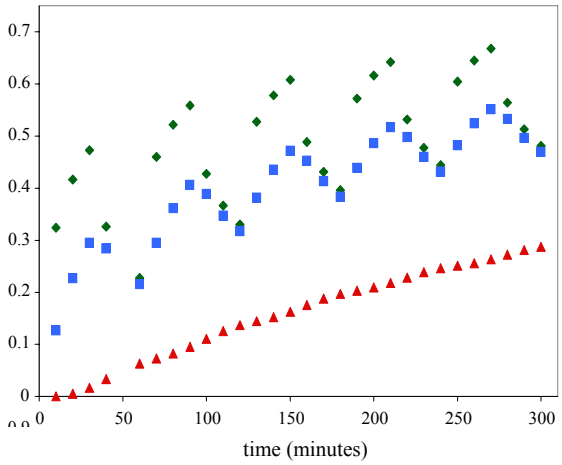

Figure 37: Simulation of photolysis and diffusion in flow cell plotted as the concentration of active growth factor relative to total growth factor as a function of time. The input rate constant for photolysis is 0.0014 s^{-1}, the experimentally determined rate constant for photolysis of light-activated EGF with 2 mW/cm^2. The diffusion coefficient is 1 x 10^{-6} cm^2/s, a typical value for a small protein diffusing in water. Photolysis (with diffusion) was carried out over 162 µm for alternating periods of 32 min. followed by 28 min. without illumination. Data are plotted as a function of time for the illuminated region (green diamonds), the adjacent 162 µm region (blue squares), and the 162 µm region starting 808 µm from the edge of the illuminated region (red triangles).

APPENDIX B
Determining Light Activation Protocol

Medium	Illumination Scheme (repeated over the course of the experiment)	Illumination Area (cm^2)	Lamp Power (mW/cm^2)	Duration	Outcome
Defined medium containing phenol red, EGF [50ng/ml]	20 hour illumination, replace medium, repeat	0.111	0.7	24 h	All cells took on spheroid morphology; many detaching. In lighted region cells appeared smaller than in other areas.
Defined Medium containing phenol red, EGF [50ng/ml]	12 hour illumination, replace medium, repeat	0.111	0.7	72 h	All cells took on spheroid morphology; many detaching. In lighted region cells appeared smaller than in other areas. Changed to medium w/o phenol red
Defined medium without phenol red, EGF [50ng/ml]	12 hour illumination, replace medium, repeat	2.27	0.7	24 h	All cells took on spheroid morphology; many detaching. In lighted region cells appeared smaller than in other areas.
Defined medium without phenol red, EGF [50ng/ml]	16 min illumination, 1 hour without illumination, repeat 4 times, replace medium, repeat	0.111	0.7	96 h	Cells maintain spread morphology, but slowly decrease in number over time
Defined medium without phenol red, EGF [50ng/ml]	5 hour illumination, replace medium, repeat	0.111	0.7	24 h	All cells took on spheroid morphology; many detaching. In lighted region cells appeared smaller than in other areas.

Medium	**Illumination Scheme (repeated over the course of the experiment)**	**Illumination Area (cm^2)**	**Lamp Power (mW/cm^2)**	**Duration**	**Outcome**
Defined medium without phenol red, EGF [50ng/ml]	90 s illumination, 60 s without illumination, repeat 4 times, replace medium, repeat	0.111	14.56	72 h	Cells maintain spread morphology.
Defined Medium without phenol red, EGF [50ng/ml]	90 s illumination, 360 s without illumination, 30 s illumination, 7 min without illumination, repeat 4 times, replace medium, wait 30 min, repeat	0.111	14.56	120 h	Cells maintain spread morphology. No higher density distribution pattern observed (*Note done with commercial EGF no pattern expected)
Defined Medium without phenol red, light activated EGF [50ng/ml]		0.111	14.56	120 h	Cells maintain spread morphology. Density distribution higher in illuminated area. Repeated 2 more times successfully
Defined Medium without phenol, light activated EGF [50ng/ml]	15 s illumination, 15 s no illumination, repeat 3 times, 15 s illumination, 58 min no illumination, repeat 4 times, replace medium, repeat	0.111	12	72 h	Cells maintain spread morphology in lighted area. Density distribution slightly higher in illuminated area, but less difference than previous illumination scheme.
Defined Medium without phenol red, light-activated EGF [50 ng/ml]	90 s illumination, 6 min without illumination, 30 s illumination, 52 min without illumination repeat 4 times, replace medium, repeat	0.111	12	120 h	Cells maintain spread morphology. Density distribution higher in illuminated area, pattern observed.

BIBLIOGRAPHY

Bakker, D. P., A. van der Plaats, et al. (2003). "Comparison of velocity profiles for different flow chamber designs used in studies of microbial adhesion to surfaces." Appl Environ Microbiol **69**(10): 6280-7.

Berneburg, M., S. Grether-Beck, et al. (1999). "Singlet oxygen mediates the UVA-induced generation of the photoaging-associated mitochondrial common deletion." J Biol Chem **274**(22): 15345-9.

Bilodeau, K. and D. Mantovani (2006). "Bioreactors for tissue engineering: focus on mechanical constraints. A comparative review." Tissue Eng **12**(8): 2367-83.

Boyden, S. (1962). "The chemotactic effect of mixtures of antibody and antigen on polymorphonuclear leucocytes." J Exp Med **115**: 453-66.

Cadet, J., Vigny, P. (1990). Bioorganic Photochemistry. New York, Wiley.

Campion, S. R., D. K. Tadaki, et al. (1992). "Evaluation of the role of electrostatic residues in human epidermal growth factor by site-directed mutagenesis and chemical modification." J Cell Biochem **50**(1): 35-42.

Chang, C. Y., B. Niblack, et al. (1995). "A photogenerated pore-forming protein." Chem Biol **2**(6): 391-400.

Curley, K. and D. S. Lawrence (1999). "Light-activated proteins." Curr Opin Chem Biol **3**(1): 84-8.

Dun, G. A. (2000). The Biomedical Engineering Handbook. Boca Raton, CRC Press.

Furuta, T., S. S. Wang, et al. (1999). "Brominated 7-hydroxycoumarin-4-ylmethyls: photolabile protecting groups with biologically useful cross-sections for two photon photolysis." Proc Natl Acad Sci U S A **96**(4): 1193-200.

Gorenne, I., R. K. Nakamoto, et al. (2003). "LPP, a LIM protein highly expressed in smooth muscle." Am J Physiol Cell Physiol **285**(3): C674-85.

Grant, M. B., P. T. Khaw, et al. (1992). "Effects of epidermal growth factor, fibroblast growth factor, and transforming growth factor-beta on corneal cell chemotaxis." Invest Ophthalmol Vis Sci **33**(12): 3292-301.

Jones, S. M. and A. Kazlauskas (2001). "Growth-factor-dependent mitogenesis requires two distinct phases of signalling." Nat Cell Biol **3**(2): 165-72.

Kim, W. J., R. R. Mohan, et al. (1999). "Effect of PDGF, IL-1alpha, and BMP2/4 on corneal fibroblast chemotaxis: expression of the platelet-derived growth factor system in the cornea." Invest Ophthalmol Vis Sci **40**(7): 1364-72.

Lin, W., C. Albanese, et al. (2002). "Spatially discrete, light-driven protein expression." Chem Biol **9**(12): 1347-53.

Luebke, K. J., Balog, R.P., Mittelman, D., Garner, H.R. (2002). Microfabricated Sensors: Applications of Optical technology for DNA Analysis. Washington, D.C., American Chemical Society.

Marriott, G. and J. W. Walker (1999). "Caged peptides and proteins: new probes to study polypeptide function in complex biological systems." Trends Plant Sci **4**(8): 330-334.

Martin, Y. and P. Vermette (2005). "Bioreactors for tissue mass culture: design, characterization, and recent advances." Biomaterials **26**(35): 7481-503.

McGall, G. H., Barone, A.D., Diggelmann, M., Fodor, S.P.A. (1997). "The efficiency of light-directed synthesis of DNA arrays of glass substrates." Journal of the American Chemical Society **119**: 5081-5090.

Miller, J. C., S. K. Silverman, et al. (1998). "Flash decaging of tyrosine sidechains in an ion channel." Neuron **20**(4): 619-24.

Peng, C.-A., Palsson, Bernhard (1996). "Cell growth and differentiation on feeder layers is predicted to be influenced by bioreactor geometry." Biotechnology and Bioengineering **50**: 479-492.

Pirrung, M. C., S. J. Drabik, et al. (2000). "Caged chemotactic peptides." Bioconjug Chem **11**(5): 679-81.

Polk, D. B. and W. Tong (1999). "Epidermal and hepatocyte growth factors stimulate chemotaxis in an intestinal epithelial cell line." Am J Physiol **277**(6 Pt 1): C1149-59.

Poujade, M., E. Grasland-Mongrain, et al. (2007). "Collective migration of an epithelial monolayer in response to a model wound." Proc Natl Acad Sci U S A **104**(41): 15988-93.

Rothman, D. M., E. J. Petersson, et al. (2005). "Caged phosphoproteins." J Am Chem Soc **127**(3): 846-7.

Ware, M. F., A. Wells, et al. (1998). "Epidermal growth factor alters fibroblast migration speed and directional persistence reciprocally and in a matrix-dependent manner." J Cell Sci **111 (Pt 16)**: 2423-32.

Zar, J. H. (1999). Biostatistical Analysis, Prentice Hall, Inc.

VITAE

Danielle Suzanne Miller was born in St. Louis, MO on October 7, 1973, the daughter of Patricia Ann Miller and Daniel Boone Miller. After graduation at Ladue High School, St. Louis, Missouri in 1992, she entered St. Louis Community College at Meramec where she received an Associate of Science degree in engineering. She then entered University of Missouri at Rolla and received the degree of Bachelor of Science with a major in Electrical Engineering in May 1997. In the years that followed, she worked as an engineer for Raytheon Systems in Waco, TX and then for Watlow in Columbia, MO. In August 2001, she entered graduate school at The University of Texas Southwestern Medical Center at Dallas in the Program in Biomedical Engineering.

Permanent Address: 18 Branford Drive
St. Louis, MO 63132